

**Neural Substrates of Spinal Sensory Integration for Reflex Control of Sympathetic
Outflow: *Where's the Connection?***

by

Rachel Susanne Bouchard

Bachelor of Science, Allegheny College 2009

Submitted to the Graduate Faculty of the
Dietrich School of Arts & Science in partial fulfillment
of the requirements for the degree of
Master of Science

University of Pittsburgh

2012

UNIVERSITY OF PITTSBURGH
DIETRICH SCHOOL OF ARTS & SCIENCES

This thesis was presented

by

Rachel Susanne Bouchard

It was defended on

November 30, 2012

and approved by

John Patrick Card, PhD, Department of Neuroscience

Linda Rinaman, PhD, Department of Neuroscience

Alan Sved, PhD, Department of Neuroscience

Thesis Director: Jon Patrick Card, PhD, Department of Neuroscience

Copyright © by Rachel Susanne Bouchard

2012

**NEURAL SUBSTRATES OF SPINAL SENSORY INTEGRATION FOR REFLEX CONTROL
OF SYMPATHETIC OUTFLOW: WHERE'S THE CONNECTION?**

Rachel Susanne Bouchard, M.S.

University of Pittsburgh, 2012

Proper adaptation to external and internal stimuli demand changes in physiology that are coordinated with motor responses. Motor responses are achieved via local circuit connections in the spinal cord and require physiological adjustments in order to be executed. Previous studies provide evidence that segmental spinal interneurons coordinate this activity. However, the identity and synaptic organization of neurons contributing to this circuitry has not been fully characterized. We hypothesize that sensory input from primary sensory afferents is integrated by local circuits that enable adaptive adjustments in sympathetic outflow through polysynaptic projections to sympathetic preganglionic neurons (SPGs) in the thoracic spinal cord. We tested this hypothesis in two experiments employing viral transneuronal tracing. In the first, a recombinant strain of PRV, either PRV263 or PRV279, was injected into the rat kidney and retrograde transneuronal passage of the virus in thoracic cord was characterized. Immunocytochemical localization of viral antigens revealed a temporally organized progression of infection through SPGs into interneuron populations in Rexed laminae VII, V, IV, II and I. Retrograde transneuronal infection reproducibly identified subpopulations of neurons in each lamina and the temporal

progression of infection was consistent with multiple parallel pathways from superficial lamina to SPGs. The second experiment utilized the expression of the farnesylated EYFP reporter that is expressed by PRV279. Localization of the farnesylated EYFP reporter defined the dendritic architecture of infected interneurons and also revealed patterns of axonal arborization coextensive with infected interneurons. Analysis of axons in both the longitudinal and transverse planes support the circuit identified in the first experiment. Both experiments reveal a segmental organization of interneurons with respect to regulation of SPG output and a neural network that appears to coordinate sympathetic outflow from multiple spinal cord segments.

TABLE OF CONTENTS

1.0	INTRODUCTION	1
1.1	AUTONOMIC NERVOUS SYSTEM	1
1.2	INTERNEURONS OF THE SYMPATHETIC NERVOUS SYSTEM.....	4
1.3	EXPERIMENTAL GOALS.....	25
2.0	MATERIALS AND METHODS	27
2.1	ANIMALS.....	27
2.2	PRV RECOMBINANTS	27
2.3	EXPERIMENTAL DESIGN	30
2.4	TISSUE PREPARATION.....	33
2.5	IMMUNOHISTOCHEMICAL LOCALIZATIONS.....	35
2.6	DATA COLLECTION AND ANALYSIS	38
3.0	RESULTS	46
3.1	CONFIRMATION OF PRV279.....	46
3.2	QUANTITATIVE ANALYSIS OF CORONAL NETWORKS	47
3.3	PRV279 ANALYSIS OF AXONAL PROJECTIONS	56
4.0	DISCUSSION	60
	LITERATURE CITED	69

LIST OF FIGURES

Figure 1. <i>The PRV Life Cycle</i>	10
Figure 2. <i>Glial Response to Viral Invasion</i>	11
Figure 3. <i>The Viral Genome of PRV</i>	29
Figure 4. <i>Renal Injection Experimental Paradigm</i>	32
Figure 5. <i>Delineation of Rexed Laminae Borders</i>	40
Figure 6. <i>Temporal Progression of Viral Labeling</i>	42
Figure 7. <i>Schematic Representation of Sympathetic Spinal Cord Segments</i>	49
Figure 8. <i>Schematic Representation of Preautonomic Viral Labeling</i>	50
Figure 9. <i>Labeling in Spinal Segment T10</i>	51
Figure 10. <i>Intersegmental Invasion of Preautonomic Networks</i>	52
Figure 11. <i>Infection of Laminae Across Thoracic Segments</i>	54
Figure 12. <i>Infection in Sensory Afferents</i>	55
Figure 13. <i>Comparison of Viral Antigen and EGFP Immunoperoxidase Staining</i>	57
Figure 14. <i>Axonal Projections in the Dorsal Horn</i>	58
Figure 15. <i>Axonal Labeling in the Longitudinal Plane</i>	59
Figure 16. <i>Schematic Diagram of Segmental Circuitry</i>	64
Figure 17. <i>Intersegmental Coordination of Sympathetic Outflow</i>	65

1.0 INTRODUCTION

Certain behavioral changes and adaptations are essential for survival of an organism and thus, its species. The evolution of this behavior makes each species adept at handling challenges of the habitat, for example, extreme cold or predation. Neural responses to sensory stimuli produce the physiological changes that occur in response to environmental challenges. These stimuli initiate adaptive motor responses that are expressed as behavior. Adaptation of an organism to the environment occurs through well-established neural circuits that generate both somatomotor (e.g., running) and physiological (e.g., respiration changes) components of adaptive behavior. These changes require precise coordination of physiological and somatomotor responses in order to be properly executed for the optimal survival. Physiological responses to challenges to homeostasis occur through adjustments of output of the endocrine and autonomic systems.

1.1 Autonomic Nervous System:

The responses of the autonomic system (ANS) are achieved through differing but complementary systems. The first system is the parasympathetic nervous system. This arm of the ANS is commonly referred to as the “rest and digest” arm. The opposing arm

of the ANS is the sympathetic nervous system and is commonly referred to as the “fight or flight” arm. These systems are defined by the effect of their activation on the organism. They can also be defined by the anatomical position of the preganglionic neurons. The parasympathetic outflow has a cranio-sacral origin while the sympathetic outflow originates in the thoraco-lumbar region of the spinal cord. However, despite the differing location of their preganglionic neurons and their functional opposition, both arms of the ANS are highly responsive to sensory stimuli and descending inputs from higher brain centers. This organization of neural circuitry is highly adaptive in that it provides a substrate for reflex responses to threatening stimuli as well as adaptation to processed sensory stimuli to restore homeostatic balance.

In the parasympathetic nervous system, the existence of such a circuit has been described by a study of the vagal system. A monosynaptic circuit from the stomach wall shows synapses from these sensory afferents in the nucleus of the solitary tract (NTS) to the vagal motor neurons in the dorsal motor vagal complex (DMV) whose dendrites extend into the NTS (Rinaman et al, 1989). In addition, there are neurons in NTS projecting to the stomach wall that do not have a primary synapse on the vagal motor neurons, indicative of a polysynaptic circuit (Rinaman et al, 1989). The parasympathetic nervous system has been described as both mono- and polysynaptic; however, the precise location of many of the interneurons has not been identified. The sympathetic nervous system has local circuit inputs, but like the parasympathetic nervous system, the location of these interneurons (Ins) has not been fully described. Similar to the parasympathetic system, much of the anatomy of the sympathetic nervous system local circuit control over sympathetic preganglionic neurons (SPGs) in

the intermediolateral cell column (IML) is understood only in general principles. There is a lack of many specific details, such as precise localization of IN populations within the spinal cord or phenotype of the circuitry.

While local circuits have yet to be fully established, there is organization of the sympathetic nervous system that is well described. Outflow originates in the IML of the thoracic and rostral lumbar cord. Preganglionic neurons are concentrated in the IML. Less dense populations of SPGs are located in the intercalatus nucleus (ICN) and the central autonomic nucleus (CAN). IML SPGs have axons that project to the para- and prevertebral ganglia and synapse upon the post-ganglionic neurons. These post-ganglionic neurons then innervate peripheral tissue (Nicholls ed. et al 2001). The cells within the IML are topographically organized, in that organs such as the kidney have their innervating pre-ganglionic neurons positioned caudal to those of the heart. Sensory afferents can alter autonomic outflow, but how these afferents access the sympathetic system at the level of the spinal cord is not well understood. There is evidence that INs play a role in this innervation using electrophysiological measures. INs within the spinal cord have the ability to fire action potentials (APs) at a faster rate than SPGs by virtue of shorter after hyperpolarization period (Deuchars et al, 2001). This fast firing rate suggests that these neurons would be able to have a large effect on SPGs. However, despite descending innervation and the location of the pre- & postganglionic neurons, the local circuits within the spinal cord have only been vaguely described.

1.2 Interneurons of the Sympathetic Nervous System:

Tract Tracing Evidence:

While interneurons within the central nervous system have been studied for decades, research on the interneurons within the thoracic spinal cord as they relate to sympathetic outflow has only more recently been researched. One of the earliest studies observing the interneuron population in the thoracic spinal cord was completed by Cabot and colleagues (1994). The research goal of the experiment was to localize interneurons in the spinal cord that are synaptically linked to the superior cervical ganglion. Injections were made into the superior cervical ganglion using wheat germ agglutinin (WGA) and cholera toxin beta subunit (CT β) either alone or in combination to identify the location of neurons antecedent to SPGs. This approach was chosen for a few reasons. First, CT β has proven to be a traditional monosynaptic tracer. This indicates that the tracer is taken up by axons, transported to the cell body and remains within that cell, without any trans-synaptic passage. Conversely, WGA has shown to be a trans-synaptic tracer, meaning that after uptake into a cell, the tracer will cross the synapse to enter a secondary neuron if present in a large enough concentration. This approach then allowed the researchers to distinguish primary or first order labeling, by presence of CT β from secondary labeling observed with WGA only.

The results showed that the primary labeling was seen in the area of the IML. The secondary neurons, or INs, were observed in Rexed laminae V and VII. In addition, Cabot and colleagues (1994) noted segmental restriction of IN labeling and thus, IN modulation is segmentally organized. This was some of the earliest evidence of a local circuit presence within the spinal cord. However, there are several key limitations to this study. The limitation with the trans-synaptic passage of WGA is that it does not self-amplify, and thus the amount of tracer seen in any secondary neurons was limited. It was unlikely to see anything further than second order connections, and that labeling is usually incomplete. Furthermore, labeling within laminae V and VII appeared in a halo like pattern around the IML which was consistent with the labeling that would be observed if the tracer had leaked from the cells. This early study identified labeled neurons in the laminae directly abutting the IML that would need to be confirmed due to these technological concerns.

The following year, Joshi et al (1995) supported this finding. Citing information from lesion studies, Joshi and colleagues became interested in interneuron networks in the spinal cord as they relate to autonomic outflow. To address the interests of the research group, Joshi et al (1995) employed the use of a trans-synaptic viral tracer to identify local circuits within the spinal cord that related to sympathetic outflow. This technique would allow labeling of INs because of the ability of the virus to self-amplify, and thus label INs to a higher degree. The experimental design used herpes simplex virus (HSV-1) as a trans-synaptic and self-amplifying circuit tracer. Using Syrian golden hamsters, the researchers injected the adrenal gland with HSV-1, Fluoro-Gold (FG), or a combination of the two. The study showed adrenal INs that were located within

laminae V and VII that showed a segmental restriction confirming, Cabot et al (1994). A morphological profile was observed for INs, differing from SPGs. SPGs had a large somatic profile that was irregular in shape (kite, elliptical, fusiform) and had large dendrite bundles that spread rostrocaudally. INs differed in that they had few dendritic branches and had smaller somatic profiles that were spherical or oval in appearance. The classification of SPG from IN was confirmed with FG and NADPH- diaphorase labeling, while neurons were separated from astrocytes with labeling for glial fibrillary acidic protein (GFAP). SPGs were identified with FG by injection of the substance into the peritoneal cavity. This has been shown to label all sympathetic SPGs (Anderson and Edwards, 1994). Additionally NADPH-diaphorase was chosen as a secondary label for SPGs due to previous knowledge of the phenotype of cholinergic sympathoadrenal neurons (Blottner and Baumgarten, 1992). Joshi et al (1995) provided data consistent with the findings of previous work and addressed the methodological concerns of the findings of Cabot et al (1994). However, due to the use of HSV-1, there are a few key limitations to the data. While interneurons were confirmed in laminae V and VII, the neurons antecedent to these interneurons may have been missed. A limited postinoculation time was essential to prevent lysis of the virus from infected cells due to the virulence of HSV-1, which limited trans-synaptic passage of virus. If a cell lysed, it would have become unclear if neurons were synaptically linked, or if the labeled cell became infected from virus in the extracellular space. While the short postinoculation time was essential for specificity, it restricted the trans-synaptic spread.

Another step towards understanding the circuitry of the local spinal circuit for sympathetic control was taken with the development and implementation of

recombinant strains of trans-synaptic neurotropic viruses. Recombinant strains are viral strains that have altered DNA to change a property of the parental virus. HSV-1 is a recombinant, which attempt to limit the virulence of the wild-type strain. The recombinant HSV-1 used in this study had an insertional mutation at a glycoprotein site to limit lysis while leaving neurotropism intact. Clarke et al (1998) used the approach that Joshi et al (1995) completed to identify non-cholinergic INs pre-synaptic to renal SPGs using a less virulent strain of HSV-1, which allowed a longer postinoculation period. Using this recombinant, Clarke et al (1998) injected the adrenal gland with virus and used an intra-peritoneal (ip) injection of the virus as a control. Using longer postinoculation periods than described previously, HSV-1 and choline acetyl transferase (ChAT) were localized within the spinal cord. ChAT was used as a marker for SPGs. Using only the data provided from the three-day post-inoculation time, populations of INs were described. The first finding was that the data were consistent with previous experiments, as INs were found in laminae V and VII. In addition, INs were also seen in the areas in which SPGs are located, the IML and nucleus intercalatus (IC). This study added to growing evidence of the location of INs, but again lacked detail in any further extension of the circuit. Only the three-day postinoculation period was included in the study, citing that the fourth day caused increased labeling that made separation of the cells in IML and IC nearly impossible. The increased infection may be due to delayed infection of SPGs or labeling of INs antecedent to SPGs within the IML that are expressing virus (Cano et al. 2004). During the time of this experiment, however, the population of INs within the IML was not well described. This study supported findings

of previous research while technological limitations prevented full labeling of the local circuits influencing sympathetic circuitry.

Technological advances helped in the location of spinal interneurons that regulate sympathetic outflow. The advancement of pseudorabies virus (PRV) in research helped to identify neuronal populations previously missed. PRV is a member of the alphaherpes family, with other viruses such as HSV (Card & Enquist, 2012). The virus is capable of infecting numerous mammals, but the natural host is swine (Card & Enquist, 2012). The wild-type strain, Becker, is extremely virulent and produces a high level of mortality. However, an attenuated strain, PRV-Bartha, was developed as a vaccine against PRV-Becker infection (Card & Enquist, 2012). This attenuated strain displays less pathogenic effects after injection, indicating a reduced virulence. Additionally, the viral spread is restricted to the retrograde direction (see figure 1; modified with permission from Card et al, 1993).

Specific deletions in the unique short (U_s) region of the viral genome are the cause of the reduced virulence, and also cause the virus to only be transported in the retrograde direction (Card & Enquist, 2012). In addition, deletion of any of the gI, gE, Us9, or Us2 loci in the U_s either alone or in combination produce reduced virulence and restricted transit in the retrograde direction (Card & Enquist, 2012). Reporter proteins have been inserted into the genome of the virus, typically at the gG locus of the U_s region. This locus, when altered, seems to have no changes in invasiveness or virulence when compared to the PRV-Bartha strain with the gG locus intact (Card & Enquist, 2012). From the PRV-Bartha strain, numerous strains have been derived displaying varying reporter proteins including EGFP, as well as genes like LacZ, which

can then be detected using immunohistochemical markers. These viruses have proven to be useful in the determination of complex circuits within the central nervous system.

Additionally, PRV invades neurons in a specific manner. First, envelope proteins on the virion have a high affinity for receptors on the axon terminal. Also, there is a temporally organized reactive gliosis to restrict non-specific spread (Card et al, 1993). After infection, astrocytes surround the infected cell. These immune cells have a high affinity for virions and prevent leakage outside of the synaptic cleft (see figure 2a) (Card et al, 1993). Importantly, there is an inability of these astrocytes to replicate and pass viral progeny. A temporally delayed clearing of infected cells occurs which prevents lysing. At late infections, microglial cells insert their processes between the pre- and post-synaptic cells and the cell is eliminated prior to lysing (see figure 2b) (Card et al. 1993). PRV strains have proven to be a specific and powerful tool to study neural circuitry.

Figure 1

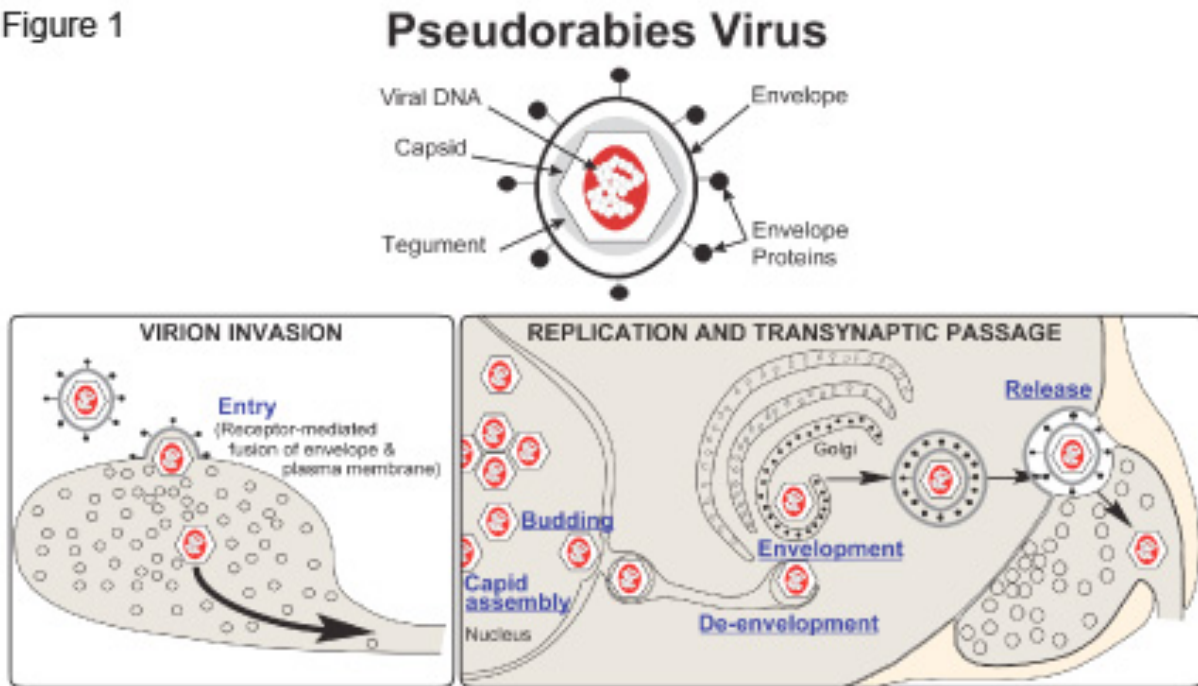


Figure 1: The PRV Life Cycle. Viral DNA is surrounded by a capsid, tegument proteins, and an envelope with envelope proteins expressed. These envelope proteins have a high affinity for receptors on the axon terminal. Upon binding to a receptor, there is a fusion of the envelope and plasma membrane of the neuron. The virus is transported retrogradely to the nucleus where viral DNA is replicated. The viral progeny then bud from the nucleus and receive two membranes on the trans face of the Golgi complex. These two membranes allow for release of the progeny into the synaptic cleft and entry into axon terminals that synapse upon the infected neuron. Adapted with permission from Card et al 1993.

Figure 2

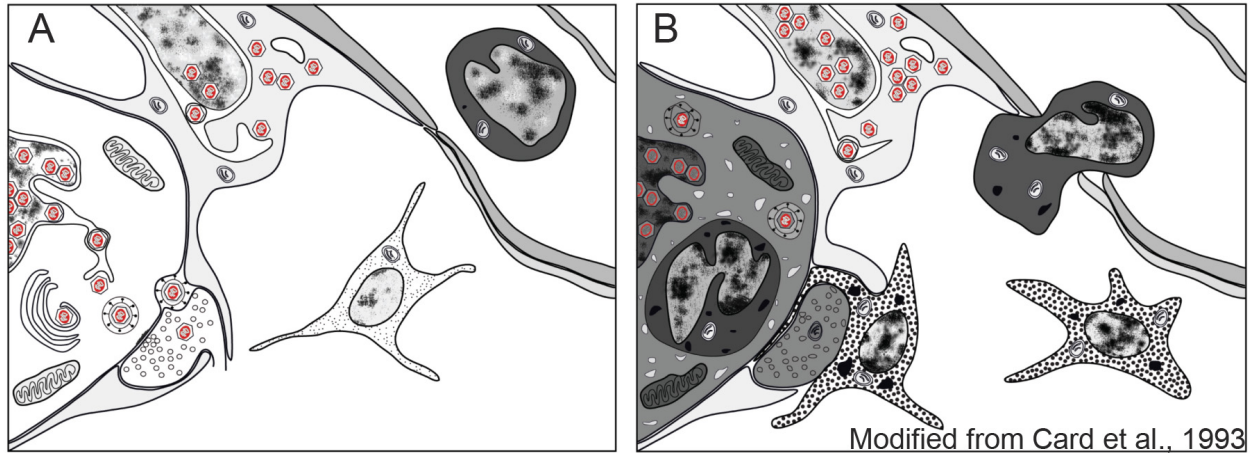


Figure 2: Glial Response to Viral Invasion. A temporally organized reactive gliosis restricts non-specific spread (A). Microglial cells insert processes between the infected presynaptic neuron and axon terminals that synapse upon it (B). Neurons that are late in viral replication are eliminated by the body's immune response.

Tang et al (2004) employed PRV-Bartha to provide greater insight into the sympathetic IN population in the spinal cord. Hydroxystilbamidin (HSB), the active ingredient in FG, was injected into the peritoneal cavity for identification of SPGs and PRV-Bartha was injected into the kidney with varying post-inoculation times observed. SPG labeling was observed in the IML to lamina X, which encompasses areas of the IML, IC, and CAN. Additionally, INs were concentrated in laminae V, VII, and to a lesser extent IV. Additionally, very limited labeling in laminae I & II was observed. These neurons were concentrated in the caudal portion of thoracic cord ranging from approximately T10-13. The study showed IN pools that had not been previously described, however, many INs may have been missed due to the short survival periods. During the time that the study was conducted, the use of PRV as a trans-synaptic tracer was still being characterized. At this time, researchers were wary of labeling within α -motoneurons and were not confident in synapse specificity of viral spread. The fear of the α -motoneurons labeling was that leakage out of the target organ may have infected axons in the neuromuscular junction, and this labeling may be indicative of a nonspecific spread of virus (Card & Enquist, 2012). This caused Tang et al (2004) to omit any cases in which there was labeling present in this population.

Only a short post-inoculation time was used because after this point, α -motoneurons were observed in the ventral horn. At a short postinoculation time point, it is possible that there was an incomplete labeling of the spinal local circuits. Since this time, more detailed studies have shown that leakage of the virus into the peritoneal cavity does not produce labeling as described previously (Card & Enquist, 2012). Additionally, hind-limb sympathectomy prior to injection of virus into the muscle showed

no labeling in ventral horn neurons of laminae VII & IX, while sympathetically intact animals showed labeling within these laminae, indicating that the labeling in the ventral horn is from a synaptic connection to the IML. If it were coming from a source other than the sympathetic nerve, invasion would have persisted after the sympathectomy. Additionally, Kerman et al (2003) has shown that injection into the areas surrounding muscle show no infection within the spinal cord motor neurons. Very limited expression of PRV within the IML was detected when the virus was injected into the area near the adrenal gland indicating the virus is unlikely to be picked up by peripheral axons when not directly injected into the target tissue.

The rostrocaudal distribution of SPGs was further described in a study by Cano et al (2001). Noting the lack of information in regards to splenic innervation, the research goal was to describe the synaptic connections of these neurons within the CNS. To identify these populations, PRV transneuronal tracing was employed. PRV-Bartha was injected into the spleen and post-inoculation times from 60-110 hours showed varying degrees of infection. In addition to the PRV injected within the spleen, a subset of animals received FG ip previous to the viral injection. The FG was used to label all somatic and autonomic preganglionic neurons (Anderson and Edwards, 1994). Results showed labeling in the left IML at T5-T9 first. As postinoculation period increased, labeling increased in density in the IML, appeared bilaterally, and was detected in thoracic segments T1-T12. The most rostral and caudal portions of thoracic cord were less densely infected than the middle, T5-T9. Later in infection, infection increased in density until the 85-hour time point. These neurons, though often found in areas containing SPGs were not labeled with FG and determined to be INs. In addition

to the description of the rostrocaudal spread of PRV, Cano et al (2001) went on to describe IN populations within the spinal cord. INs were observed in all areas where SPGs are located, including IML, IC, and the central autonomic nucleus (CAN). INs were seen above and below the IML in a horizontal plane, in regions that are likely to be laminae V & VII. Additionally, Cano et al (2001) described populations infected within the brain at early infection times. Supraspinally, neurons were seen labeled in the A5, region, ventral medial medulla (VMM), paraventricular nucleus of the hypothalamus (PVN) and the rostroventral lateral medulla (RVLM) among others. These populations are described to be monosynaptic to the sympathetic SPGs and are some of the earliest regions infected after sympathetic injections of PRV. Since this study, the infection of these regions has been used as a marker to determine the temporal progression of viral infectivity. This experiment provided valuable data in regards to autonomic circuitry. However, the plane of section used limits specificity of the laminar location of infected populations. Also, novel PRV recombinants have been subsequently developed and provide increasing power to delineate complex neural circuitry.

In a subsequent study, Cano et al (2004) used a dual injection paradigm to analyze the use of PRV as a tracer for a more complex circuit analysis. PRV-BaBlu and PRV-152 were injected in opposing kidneys. This approach allowed for identical innervations to be observed to both confirm the ability for a neuron to display infection of both viruses as well as demonstrate dual localization of unique reporters to identify neurons innervating both kidneys. This approach showed numerous populations within the brain that had both single and double-labeled neurons. This finding proves that neurons can be co-infected and also shows circuitry within the brain for coordinated

renal outflow. In addition to supraspinal circuits, Cano et al (2004) described spinal circuits and confirmed the previously published findings showing labeling in lower thoracic cord IML initially, before spread to INs within IML, IC, and CAN. It was also shown that INs were localized within laminae V & VII. Few single and dual-labeled neurons were observed in laminae I & II. The plane of section and limited number of neurons observed in these laminae at the times analyzed only provide a suggestion of a spinal circuitry that extends into the superficial dorsal horn. Importantly, this study is one of the earliest to indicate that dorsal horn neurons are involved in the synaptic circuitry of kidney regulation.

Electrophysiological Evidence:

Interneurons within the IML, as well as adjacent to the IML, have also been described physiologically. While INs in the brain have been shown to have a fast firing frequency and shorter inter-spike interval (ISI), those within the spinal cord have yet to be described. Using the knowledge of the presence of specific voltage gated potassium channels, Deuchars et al (2001) aimed to describe INs that may be able to alter the activity of the SPGs based on their anatomical position and description of IN pools from earlier experiments (Cabot et al 1994; Joshi et al 1995). The experiment involved thoracic spinal cord slices of young rats to record from neurons adjacent to the IML. These neurons were hypothesized to have a different physiological profile than the SPGs in the IML. The INs recorded were shown to have a shorter interval from rising potential to the bottom of the after hyperpolarization (AHP) as well as an increased firing

frequency. These properties were abolished after administration of two chemicals, TEA and 4-AP, which have been shown to inhibit the Kv3.1b and Kv3.2 channels implicating these channels in the unique properties of the INs around the IML. After recording from these neurons, Deuchars et al (2001) used electron microscopy to observe synaptic connections. FG was administered ip and these sections were stained for this tracer and Kv3.1b, which was chosen based upon the presence of this protein in the spinal cord. Importantly, neurons that were FG+ did not contain the potassium channel subunit, while those that did contain the channel did not show FG labeling. This indicates that the channel subunit is on INs that synapse upon SPGs. The SPGs lack the potassium channel subunit. In a subset of recorded INs filled with Lucifer yellow, it was shown that those neurons that contained the marker also were Kv3.1b+. This study showed a physiological marker of INs that are positioned in an ideal location for IN innervation and modulation of SPG activity.

In a subsequent study from the Deuchars group, Brooke et al (2002) linked the SPGs from the adrenal gland with INs containing the Kv3.1b channel. In this experiment, the adrenal gland was injected with a HSV recombinant that expresses a green fluorescent protein (GFP). To identify SPGs, FG was also injected ip a week prior to the HSV injection. The use of the trans-synaptic tracer allowed the ability to synaptically link the INs that expressed the Kv3.1b subunit with SPGs that innervate the adrenal gland. The INs that expressed the subunit were located within the IML as well as immediately surrounding it. This study showed IN populations that were electrophysiologically distinct and synaptically connected to the adrenal gland.

Correlation of activity between spinal cord dorsal horn neurons and sympathetic neurons was described by Chau et al (1997). Activity persists in the spinal cord after spinal transection and therefore may be an important step towards treatment after spinal cord injury. Therefore, it may be an important source of afferents to the SPGs both in the spinalized as well as intact animal. To address this lack of knowledge, Chau et al (1997) performed spinal transection of male Sprague-Dawley rats at the level of C1-C3. After spinalization, one of five different areas of thoracic or lumbar cord was exposed for recording including T2, T8, T10, T13, and L2. In addition, the renal sympathetic nerve was exposed for recording of renal sympathetic nerve activity (RSNA). After placement of recording electrodes, an innocuous (cotton-tipped applicator brushed across skin) or noxious (pinch with toothed forceps) stimulus was administered to the corresponding dermatomes. Neurons were characterized based on the stimuli to which they responded using the classification of low threshold (LT), high threshold (HT), wide dynamic range (WDR) or other if they did not respond, or responded by decreasing RSNA. Correlated neurons were located in lower thoracic (T10) laminae V, IV, and III. The dorsal horn neurons exhibited a bursting pattern similar to RSNA. They were also nearly all WDR. These neurons are physiologically linked to sympathetic activity; however, the precise circuitry of their synaptic connections was not described. While recording from these neurons that were correlated is important, other neurons may have been omitted based on inclusion criteria.

Following the description of dorsal horn neurons and the correlation to RSNA, Chau et al (2000) went on to characterize the neurons of the intermediate zone and

their correlation to RSNA. The intermediate zone is an area that is located between the IML and CAN. There have been studies that have shown a prospective population of INs for presympathetic neuron regulation within this region (Cabot et al, 1994; Schramm et al. 1993). Methodologically, the experiment followed the procedures of an earlier study (Chau et al, 1997), but included a stimulus that was clinically relevant. In order to confirm their findings, as well as add new knowledge to the literature, the group completed the acute spinal transection, recorded from T10 INs and the renal nerve, and completed innocuous and noxious stimuli on the T10 dermatome. The study found two differing populations of correlated neurons in the intermediate zone. The first, responded similarly to the WDR dorsal horn neurons described previously (Chau et al 1997) in that they fired to the innocuous stimulation and increased from that firing to noxious stimuli. The other half of the intermediate zone neurons responded in a way that was very different from these neurons. The innocuous stimulation caused an increase in firing of these neurons like the WDR, however the noxious pinch to the T10 caused a decrease in firing, while a pinch outside of the T10 dermatome would cause an increase in firing. This suggests that these correlated intermediate zone neurons have a differing afferents than those of the dorsal horn neurons or WDR intermediate zone neurons.

In addition to the description of the intermediate zone correlated neurons, Chau et al (2000) determined the effect of colorectal distension (CRD) on the firing of the dorsal horn neurons and intermediate zone neurons that were correlated to RSNA. CRD increases RSNA and it was hypothesized that these correlated spinal neuron populations may be implicated in this circuitry. Chau et al (2000) hypothesized that the

correlated neurons would increase in firing frequency as suggested by previous research. Dorsal horn neurons, however, were inhibited by CRD, while intermediate zone populations were excited by CRD. The effects of CRD on the local circuits indicated by correlative findings in electrophysiology are of interest. It is hypothesized that there is a segmental organization and these two populations cause the effect of CRD on RSNA. A combination of a segmental input from correlated dorsal horn neurons and the intermediate zone would then alter the activity of the SPGs to the CRD. This integration of inputs across segments remains to be described in detail.

Subsequent to Chau et al (2000), other researchers have observed IN activity in intact animals, as most research previously has been in spinalized animals. This research was aimed at determining if the effects described previously are due to spinal transection and are not present in an intact animal (Miller et al 2001). After exposure of the T10 region and the renal nerve, stimulation was completed in the rostral spinal cord. This study used the upper cervical region for stimulation to compare the data with that previously described by their laboratory. It was determined that there were less renally correlated neurons in the intact animal than had been described in previous spinalization literature. Miller et al (2001) noted that the discrepancy between the two conditions might be due to supraspinal modulation. This local circuit input may have the ability to drive the sympathetic innervation, but is inhibited by supraspinal input in the intact animal. Despite the advances of using the intact animal, the cross-correlation method may have omitted neurons that show a weaker correlation with RSNA. Also, neurons were recorded at several depths from the dorsal most edge of the dorsal horn to the ventral edge of the intermediate zone, however no anatomical localization was

described. The lack of anatomical descriptions left any potential synaptic links that may be demonstrated using immunohistochemistry still not described.

INs that are sympathetically correlated have also been described by Tang et al (2003). The goal of the electrophysiological study was to better identify and understand the spinal INs that are responsible for sympathetic drive following spinal injury (Tang et al 2003). Additionally, the anatomical location of somata and reconstruction of dendrites had yet to be described. The location of these neurons is important to consider when determining a population's likelihood to receive primary afferent innervation, or if the majority of innervation originates supraspinally. To address this gap in knowledge, animals received spinal transection at C2, and recordings were completed at T10. RSNA was recorded and relationships between action potentials and RSNA were correlated. Subsequent to recording, neurons were filled with biotinamide for reconstruction of the neurons. Electrophysiologically, neurons correlated with RSNA were shown in numerous laminae of the spinal cord. Somata were seen as far dorsal as lamina I, and recorded in all dorsal horn laminae (Tang et al 2003). The majority of neurons were recorded from lamina IV with fewer located in the other laminar divisions (Tang et al 2003). The dendrites of INs recorded were shown to have branching dendrites that extended both mediolaterally as well as dorsal ventrally between many laminae of the dorsal horn. The study showed the morphology and anatomy of previously described populations in greater detail.

Functionally, INs within the spinal cord have been implicated in the regulation of sympathetic activity. The majority of the research in the field of local circuit regulation is due to the presence of autonomic dysreflexia after spinal cord injury. Autonomic

dysreflexia is a life threatening condition in which, normally innocuous stimuli, such as a light brush, causes changes in sympathetic outflow, such as increases in arterial pressure and bradycardia among others. This can be life threatening due to the increased likelihood of cardiac arrest or stroke (Krassioukov et al 2002). This condition is most common in patients with upper thoracic or cervical injuries. Despite the prevalence of this condition after spinal cord injury, very little is known about the circuitry involved.

To begin to understand the circuits involved, Krassioukov et al (2002) aimed at determining any differences in correlated INs within the dorsal horn of the spinal cord between acute and chronically spinalized animals. Spinal cords were transected at T3, and either recorded from immediately for acute condition, or after 1 month for chronic condition. Recording methods were previously described by their laboratory and were employed in this experiment (Chau et al 1997, Chau et al 2000). The addition of colorectal distension data was essential for the study. Autonomic dysreflexia can be caused by numerous stimuli including bladder distension and CRD. This relevant stimulus was an ideal choice when studying this circuitry as it made the findings more clinically relevant. After recording from the two separate groups of spinalized animals, it became apparent that the spinal cord undergoes plastic changes after injury. After chronic spinal transection, more numbers of neurons were excited in areas stimulated with the noxious and innocuous stimuli when compared with an acute transection. Additionally, the neurons that were correlated with RSNA after chronic spinalization were more responsive to stimulation than the INs correlated in the acute spinalized animals. With regards to the CRD recordings, chronically spinalized animals had a

larger change in mean arterial pressure than acute spinalization. INs in the two groups did not differ in their responses to changes in arterial pressure. Therefore, while peripheral conditions were different, cell physiology did not change. Taken together, Krassiouov et al (2002) demonstrated the plasticity of the local spinal circuit and changes in sympathetic regulation after chronic spinalization.

In addition to functional and anatomical support for a spinal circuit regulating autonomic outflow, physiological data also support an inhibitory node between forebrain and SPGs. Citing physiological evidence in which stimulation of the medial prefrontal cortex sends a glutamatergic projection to CAA, but decreases sympathetic outflow as shown by hypotension, Deuchars et al (2005) aimed to identify GABAergic neurons within the spinal cord CAN. PRV-BaBlu was injected into the adrenal gland. Immunohistochemical localization of PRV and *in situ hybridization* for GAD65 & GAD67 were completed to identify the population. Neurons in the CAN that were shown to be presynaptic to SPGs were also GABAergic, containing GAD65, but rarely GAD67. Additionally, stimulation of the CAN region shows a monosynaptic IPSP in the SPGs. This possibility of modulation of SPGs allows another node of modulatory influence for fine tuned adjustments of the circuit. This research proposed a circuit that provides an opportunity for excitatory input to the INs that can prepare the sympathetic nervous system for a challenge and decrease functioning.

Spinal Transection Study Evidence:

The persistence of afferents after spinalization to the SPGs has been examined to determine the possibility of local sources of afferents of various neurotransmitters and neuromodulators. Llewellyn-Smith et al (2005) specifically described a population of INs that contains enkephalin (ENK). ENK was specifically chosen due to the effects of opioids on suppression of micturition reflexes as well as the presence of enkephalin terminals near sacral preganglionic neurons that disappear after spinal transection. This peptide was hypothesized to be mainly from supraspinal projections. After injection of Ct β into the major pelvic ganglion of the rat, terminals that were ENK+ were analyzed for their proximity to pelvic related preganglionic neurons. To address the origin of these terminals, intact cords were compared with those that were transected either 2 or 11 weeks prior. At the light microscopic level, varicose ENK+ fibers appeared in high quantities around the Ct β + cells and dendrites. This dense labeling of ENK around Ct β + cells persisted after transection, indicative of a spinal source of this peptide. At the electron microscopy level (EM) this close apposition of fibers and cells/dendrites were confirmed to be synapses. Taken together, Llewellyn-Smith et al (2005) noted endogenous opioids may modulate pelvic outflow, and these opioids originate locally, rather than supraspinally.

In addition to ENK, Llewellyn-Smith et al (2007) showed other neurotransmitters that originate in the spinal cord for autonomic regulation. With the development of markers for the vesicular transporter for glutamate (VGLUT1 & VGLUT2), the ability to distinguish glutamate neurons from others that use glutamate in everyday functioning or

as a precursor for GABA became possible. Using the same approach as in a previous publication (Llewellyn-Smith et al, 2005), Llewellyn-Smith et al (2007) aimed at determining the input of glutamate to SPGs and the origin of the glutamate fibers. Intact cords were analyzed for location of VGLUT1 & 2 populations, as the marker had recently been developed and these populations were not yet known. Determining the location of these transporters within an intact spinal cord showed VGLUT1+ terminals in the dorsal horn and medial portions of laminae IV, V, & VII, including the dorsal nucleus of Clarke. VGLUT2 was present in the entire spinal cord with omission in the dorsal nucleus of Clarke. More importantly, Llewellyn-Smith et al (2007) noted a differentiation of VGLUT innervation between SPGs and INs. VGLUT2 was mainly seen in areas of autonomic preganglionic neurons. VGLUT1 was mainly seen targeting areas of INs within the spinal cord. In addition, comparison of the intact and transected rats showed VGLUT2 remaining present after chronic transection. Interestingly, VGLUT1 increased in density in the parasympathetic regions after spinal transection. It is feasible to hypothesize that this increase is due to the plasticity of the system and possible increases in sensory input to these regions.

Sympathetic control is also altered by GABAergic innervation. After discovery of perisynaptic GABA receptors, tonic inhibition was described that could change the excitability of dentate granule cells (Otis et al, 1991). The description of a channel outside the synaptic cleft that alters excitability provided a new avenue of research. These receptors may be present on SPGs and be positioned to modulated sympathetic outflow (Wang et al, 2008). GABA has been implicated in sympathetic regulation because of the effects of GABA_A receptor antagonists on arterial pressure. (Marty et al.

1986; Taneyama et al, 1993). Because of this research on the GABA_A perisynaptic receptors, Wang et al (2008) aimed to determine if these receptors are present on SPGs using electrophysiological measures. Upper and middle thoracic spinal cord slices were used for recording. Specific GABA_A and GABA_B receptor antagonists were administered as well as various modulators to determine the receptor identity in these populations. Using physiological markers of INs vs SPGs, Wang et al (2008) demonstrated that the neurons responsive to GABA were SPGs and not INs. Additionally, these GABAergic receptors when stimulated, decreased the SPG firing rate and, when inhibited, SPG activity increased (Wang et al. 2008). This study described another source of input regulating sympathetic outflow, however, the population providing this input remained unknown. An important finding of Llewellyn-Smith et al (1997) and Llewellyn-Smith & Weaver (2001) demonstrated that GABA and glutamate terminals remain present after chronic spinal transection, indicating that these neurons receive at least some of their amino acid input from local spinal circuits.

1.3 Experimental Goals:

Despite numerous attempts at fully describing the spinal circuitry as it relates to sympathetic outflow, there is still limited data on the subject. Phenotypically, there is evidence of a spinal circuit with GABA, glutamate, and neuropeptides present. Physiologically, evidence exists for a population of INs that have activity which correlates with RSNA. Anatomically, there have been numerous studies to show neurons within laminae V & VII with more limited information on IV, III, II, and I.

However, the spinal cord local circuit may not be fully characterized due to technological concerns. More thorough descriptions of trans-synaptic viral tracers, as well as development of novel strains of virus provide the ability to better illustrate the axonal links between populations of infected neurons. Using a novel strain of PRV, PRV-279 that expresses a farnesylated yellow fluorescent protein reporter, axons will be localized and present a better description of the circuitry involved in transneuronal labeling and communication. This farnesyl group is a neutral compound, which, by nature, is hydrophobic. This causes the protein to be placed into the lipid bilayer of the membrane. The location of the fluorescent reporter in the membrane causes the entire neuron to be labeled including distal dendrites and axons. Additionally, the use of a PRV recombinant, PRV-263, which expresses the Brainbow 1.0L cassette will aid in confirmation of viral labeling in the dorsal horn neurons. The Brainbow virus has been discussed in detail in Card et al (2011) and will be reviewed in the following section. Injections will be in the kidney which is a model system that has been well defined in our laboratory (Cano et al, 2004; Card et al 2011). INs can be differentiated from SPGs with FG labeling which was injected ip 1 week prior to kidney injection (Cano et al. 2001, Cano et al. 2004). The goal of the experiment is to more fully describe the spinal circuits, both segmentally and intersegmentally, as they relate to autonomic outflow. It is hypothesized that sensory information is relayed to SPGs through a circuit within the dorsal horn. This may occur either in parallel or sequentially, and employing viral transneuronal tracing, as well as a novel strain of PRV, the goal is to more thoroughly define this circuitry.

2.0 MATERIALS & METHODS

2.1 Animals

Adult male Sprague Dawley rats (220-260g, Charles River) and adult male C57BL/6J mice (18-26 g, Jackson Labs) were used in this investigation. Animals resided within a laboratory certified for BSL2 experiments throughout the duration of the study. Photoperiod (12:12 light/dark cycle; light on at 0700) and temperature (22-25° C) were standardized. Animals had free access to food and water. All experiments conformed to regulations stipulated in the NIH Guide for the Care and Use of Laboratory Animals and the CDC-NIH Biosafety in Microbiological and Biomedical Laboratories (HHS Publication No. 88-8395). The Institutional Animal Care & Use Committee, the Institutional Biosafety Committee, and the Environmental Health & Safety Department at the University of Pittsburgh approved all experimental protocols.

2.2 PRV Recombinants.

Pseudorabies Virus (PRV) is a swine α -herpesvirus. An attenuated vaccine strain (Bartha) has been used for numerous studies and has been well characterized by our laboratory. In brief, the genome of the virus has a unique long (U_L) and a unique short (U_S) region. Mapping the genome has revealed point mutations and deletions in both regions of PRV-Bartha compared to the wild type Becker strain. These deletions make the virus less virulent and also prevent the virus from transporting in the anterograde

direction, only permitting spread in the retrograde direction (Card & Enquist, 2012). These tracers provide a way to trace multi-synaptic circuits that is self-amplifying and labels the circuit more completely than traditional tracers (Card & Enquist, 2012).

All of the viruses used in this analysis are recombinants of PRV-Bartha. PRV-263 is a virus that was created from PRV-152 and has been previously described in detail (Kobiler et al, 2010). In brief, homologous recombination replaced the EGFP reporter gene at the gG locus with the pBrainbow1.0L cassette generated by Lichtman and colleagues (Livet et al, 2008). The cassette codes for three fluorescent reporter proteins; dTomato, EYFP and mCerulean. Prior to recombination, the default fluorophore profile is dTomato. After contact with cre-recombinase, the yellow (EYFP) or blue (mCerulean) reporter is expressed due to excision of the red reporter gene, either alone or in combination with the EYFP gene (see figure 3). This is achieved by Cre-mediated recombination at either the paired loxP or lox2272 sites. In the current investigation the Cre-mediated recombination capabilities of the virus were not used and only the dTomato reporter protein was expressed.

Figure 3

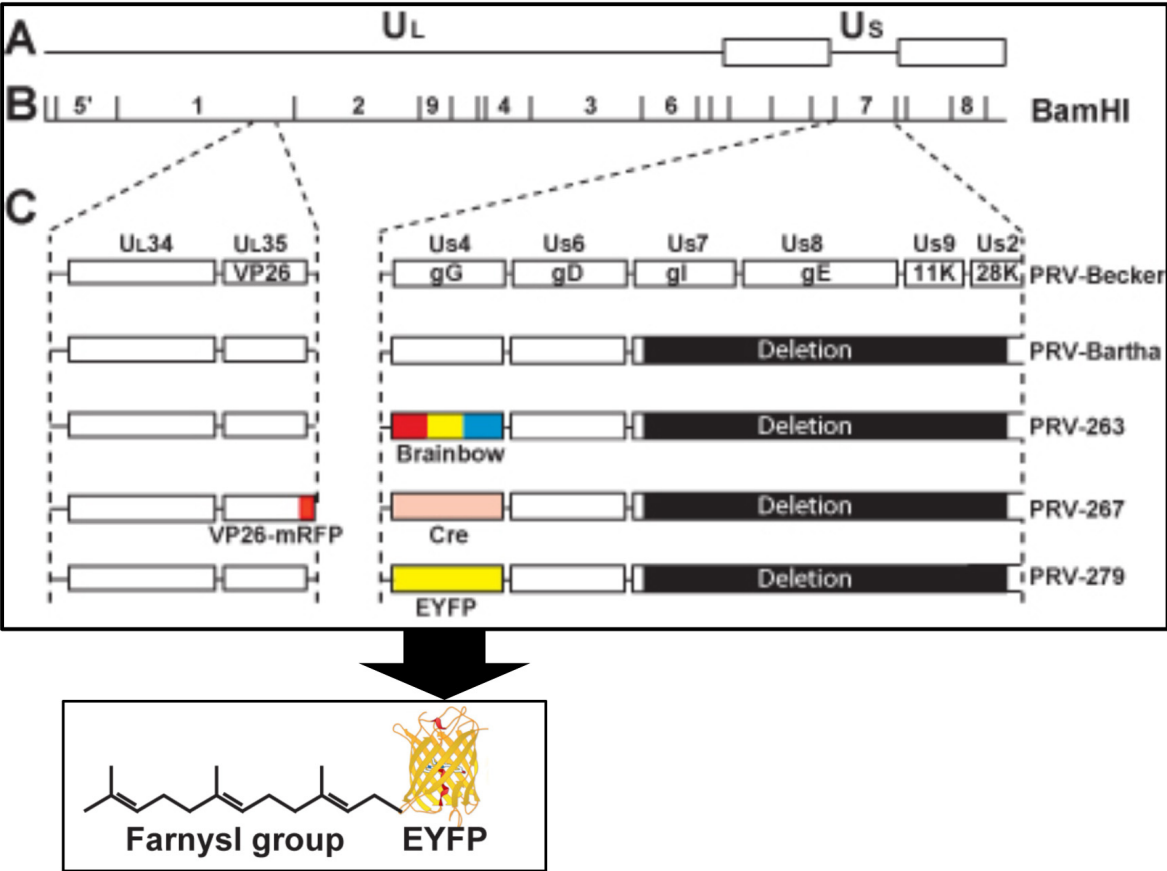


Figure 3: The Viral Genome of PRV. The DNA of pseudorabies virus has a unique long (U_L) and a unique short (U_S) region (A). The restriction map of the viral DNA is illustrated (B). The attenuated, PRV-Bartha, strain shows a large deletion in the U_S region that causes the virus to become less virulent, maintain neurotropism and restricts transport to the retrograde direction. Reporter proteins have been inserted into the gG locus. Recombinants, PRV-263 and PRV279 with the Brainbow 1.0L cassette and a farnesylated EYFP reporter in the gG locus respectively were used in this study (C).

PRV-279 was generated for this study. The virus was generated by Cre-mediated recombination of another “Brainbow” recombinant – PRV-271. The Brainbow 1.1M cassette in the gG locus of PRV-271 contains the Korange, mCherry and YFP genes in sequence, separated by loxP and lox2272 sites. Korange is the default reporter of this virus in the absence of the bacterial enzyme cre recombinase (Cre). In the presence of Cre the Korange gene is recombined from the cassette, either alone or in combination with the mCherry gene. This Cre-mediated recombination generates strains of virus expressing either mCherry or YFP. Importantly, the mCherry and YFP genes are farnesylated. Attachment of the hydrophobic farnesyl group to the fluorescent reporters results in their insertion into the plasma membrane of infected cells (see figure 3). PRV-279 was produced by growing PRV-271 on Cre-expressing PK15 cells and then isolating plaques only expressing the YFP reporter.

2.3 Experimental Design.

Rat Procedure. Animals were anesthetized with 2% isofluroane in oxygen. Once a pedal response was absent, animals were placed on their side to expose the flank. Fur was removed with an electric shaver and cleared via suction. The exposed skin was sterilized with betadine. An incision was made below the rib cage to expose the abdominal musculature. Muscle was cut with surgical scissors and the peritoneum was pierced to gain entry into the abdominal cavity. The kidney was exposed using cotton swabs and gently removed from the abdominal cavity to the body surface for injection taking care to prevent damage to the tissue.

Once exposed, the kidney was injected with the PRV virus. Injections were made using a 10 μ l Hamilton syringe. The needle of the syringe was marked at 4 mm to ensure constant depth of injections into the parenchyma. After kidney exposure, the syringe was freshly loaded with the virus. The kidney was injected at 4 sites. Each injection was made from the greater curvature towards the hilus. Volume for each site was 0.5 μ l with the total volume injected equaling 2 μ l. The injections were completed using microscopic observation. The needle was left in place for approximately 2 minutes following each injection to reduce reflux from the needle tract. Any reflux or bleeding from injection sites was absorbed with cotton swabs (see figure 4).

Once all injections were completed, the kidney was gently placed back into the peritoneal cavity. Muscles were sutured using non-absorbable sterile sutures. Skin was closed using surgical staples. Animals received a subcutaneous injection of analgesic (Ketofen, 2 mg/kg) and were returned to their home cage following recovery of consciousness and its ability to attend to bodily needs. Each animal was monitored daily for any signs of sickness or distress including spiked fur, nasal discharge, and weight loss.

Mouse Procedures. Surgeries were completed in the same way as the rat surgeries with alterations made to accommodate the smaller size of the mice. First, the Hamilton syringe was fixed with a pulled glass micropipette tip to limit the damage to the tissue. Next, a total volume of 1 μ l of virus was split between two injection sites. Skin was also closed with sterile sutures. Animals were weighed daily, as visual signs of sickness were less apparent in this species.

Figure 4

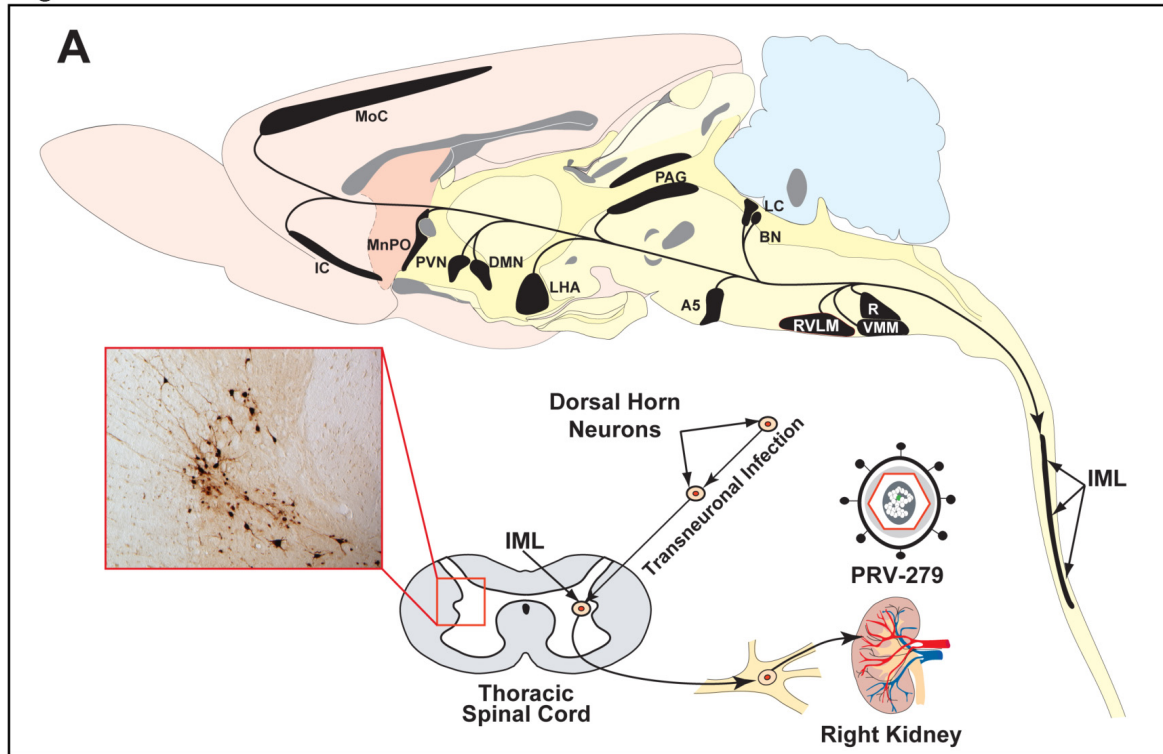


Figure 4. Renal Injection Experimental Paradigm. Virus was injected into the kidney at a depth of 4 mm into four sites. Transport through the ganglia to the SPGs in the IML and then transneuronally to the dorsal horn and supraspinally are localized using viral reporters or immunocytochemical localization of viral proteins.

2.4 Tissue Preparation:

At the designated post inoculation survival interval deeply anesthetized animals were perfused and the brain and spinal was collected for immunocytochemical analysis. Anesthesia was achieved with an overdose injection of Fatal Plus into intraperitoneal cavity (0.2 ml/rat, 0.1 ml/mouse of 390 mg/ml solution based upon sodium pentobarbital concentration; Butler Schein). The absence of a pedal withdrawal reflex was the criterion used to determine an acceptable level of anesthesia. Rats were perfused transcardially with 100 ml 0.9% physiological saline followed by 300 ml of 4% paraformaldehyde-lysine-periodate solution (PLP; McLean & Nakane, 1974). Mice were perfused using the same solutions but with 20 ml of 0.9% physiological saline and 100 ml of PLP fixative. Brains and spinal cords were removed and placed in PLP solution overnight at 4°centigrade. Tissue was then placed in 20% followed by 30% phosphate buffered sucrose solution overnight or until tissue had sunk to the bottom of the container.

Spinal cords used for coronal analysis (n=15 rats, n=2 mice) were removed by performing a dorsal laminectomy. Cervical vertebra 1 was removed first, cutting the spinal cord from the brain at the rostral edge of the opening of the first cervical vertebrae. Next, dorsal rootlets were identified with microscopic assistance and cuts were made directly caudal to the rootlet entry. Segments were removed after each cut and collected into individual wells containing PLP fixative for post-fixation. Brains were also collected by removal of the skull and severance of the cranial nerves.

Spinal cords used for horizontal analysis (n=4 rats, n=9 mice) were removed by performing a dorsal laminectomy through the entire rostrocaudal extent of the cord.

Spinal nerves were severed and the cord was removed in one piece. The cord was cut into three segments for microtome sectioning and tissue analysis. Proximal, intermediate, and distal segments, determined by enlargements at the cervical and lumbar regions of the spinal cord, approximated cervical, thoracic, and lumbosacral portions of the cord respectively. A fiducial mark was made in the rostral right portion of the cord for orientation.

Dorsal root ganglia (DRG) were collected from rats that were included in the horizontal analysis (n=2, 96h post-inoculation time). Ganglia were identified by following each spinal nerve from the cord through the vertebral column under microscopic observation. DRGs were collected in individual wells, noting thoracic segment to which they were connected as well as side of the body.

All tissue was post-fixed overnight in PLP fixative. Following postfixation tissue was cryoprotected by sequential changes of 20 and 30% phosphate buffered sucrose at 4° C. Adequate cryoprotection was determined by tissue sinking to the bottom of the container. The brain was cut at 35 μ m and collected in 6 bins of a glycol-based cryoprotectant (Watson, et al, 1986). The spinal cords, regardless of plane of section, were sectioned at 40 μ m in 4 bins. Brain and spinal cords were cut using a freezing stage sliding microtome. Tissues were stored in cryoprotectant (Watson et al, 1986) at -20° C until the time of processing. DRGs were sectioned using a cryostat at 20 μ m in a 1:4 series and placed directly onto Fisherbrand Superfrost slides for fluorescent analysis.

2.5 Immunohistochemical Localizations

Immunohistochemical Reagents: Rabbit polyclonal antisera generated against acetone-inactivated PRV (Rb132 and Rb133) identified viral antigens in infected neurons (1:10,000 peroxidase dilution; Card et al 1990). EYFP was localized using a chicken α -EGFP antibody that cross-reacts with EYFP (1:10,000 peroxidase dilution; AbCam, Cambridge, MA). Secondary antibodies used in the study were donkey anti-rabbit, Cy2 conjugated donkey anti-rabbit, and Cy3 conjugated donkey anti-chicken (Jackson ImmunoResearch Laboratory; West Grove, PA).

Immunoperoxidase Localizations: Immunoperoxidase localizations were completed for all antibodies in the same manner, selecting the primary antibody and complementary secondary antibody to localize the desired protein. First, free-floating tissue was washed for 30 minutes in 10 mM phosphate buffered saline (PBS) at 10 minutes/wash in a mesh well. The tissue was then transferred to 100 ml of 0.5% sodium borohydride in 10 mM PBS for 10 minutes to break aldehyde bonds. Following sodium borohydride treatment the tissue was washed in multiple changes of 10 mM PBS to completely remove sodium borohydride. The tissue was then incubated in a methanol-hydrogen peroxide solution for 10 minutes to reduce background staining, washed in 3 changes of 10 mM PBS over 30 minutes, and placed into primary antibody for incubation overnight at room temperature. Primary dilutions were achieved using a mixture of antibody, 10

microliters (ul)/1 ml of normal donkey serum, 30 ul/ml of 10% TX-100 and 0.1 M sodium phosphate buffer (PO_4 , pH=7.2) to reach 1 ml of the diluted antibody solution.

After incubation, tissue was washed in 3 changes of 10 mM PBS over 30 minutes for removal of unbound antibody. Tissue was placed in a biotinylated secondary antibody (1:200 donkey anti-rabbit or donkey anti-chicken; Jackson ImmunoResearch Laboratories, West Grove, PA) for 60 minutes. Sections were subsequently washed in buffer prior to and following incubation in an avidin-biotin complex solution (Vectashield ABC *Elite* 5 ul of each reagent combined for 90 minutes before incubation, Vector Laboratories, Burlingame, CA) for 90 minutes. Tissue was then placed in a solution of 0.1 M Tris-buffer saturated with diaminobenzadine (DAB) for 10 minutes before addition of 35 ul of H_2O_2 per 100 ml 0.1 M Tris buffer to generate the brown reaction product. The DAB reaction was terminated after 5 minutes tissue by washing the tissue in multiple changes of PBS buffer. Sections were mounted on Fisherbrand Superfrost microscope slides (Fisher Scientific, Pittsburgh, PA), dehydrated using a graded ethanol series, cleared in xylenes, and coverslipped using Cytoseal-60 (Richard-Allan Scientific, Kalamazoo, MI).

Immunofluorescence Processing:

Fluorescent reporters were visualized by their natural fluorescence or by enhancement with antibodies. Antibody enhancement was achieved through incubation of tissue in chicken antisera generated against EGFP at 10X the concentration used for immunoperoxidase. First, the cryoprotectant was washed from the tissue using three 10 minute washes in 10 mM PBS. Tissue was incubated in 0.5% sodium borohydride to

break aldehyde bonds. The sodium borohydride solution was then removed by several washes changes of 10 mM PBS for at least 30 minutes, or until all bubbles were absent from the solution. Following this wash, a methanol-hydrogen peroxide wash was completed to reduce background staining. Tissue was then washed of this solution for 30 minutes at 10 minutes a wash. Incubation in a primary antibody, chicken α -EGFP (AbCam) took place overnight at room temperature at a dilution of 1:1000, diluted with 0.1 M PO_4 buffer, TX-100, and normal donkey serum.

The following day, tissue was washed of unbound primary antibody in several changes of 10 mM PBS for one hour. Tissue was then incubated in Cy-2 conjugated donkey α -chicken, which recognizes the primary antibody and attaches a fluorescent tag, for 120 minutes at room temperature under a cover to limit light exposure. Again, dilution consisted of normal donkey serum, TX-100, and 0.1 M PO_4 buffer. After incubation, tissue was thoroughly washed in 10 mM PBS. Following the wash, tissue was mounted onto Fisherbrand SuperFrost microscope slides. Slides were allowed to dry overnight in a 4° centigrade refrigerator in a closed slide holder. Slides were then passed through graded ethanol and xylenes, at reduced wash times, before coverslips were applied with Cytoseal-60 (Fisher Scientific; Pittsburgh, PA). Incubation in secondary antibody and all subsequent steps were completed with limited light exposure to prevent any potential bleaching of the fluorescent reporter.

Dual fluorescent localization was achieved through a similar process with a few key changes. The pretreatment with sodium borohydride and methanol-peroxide solutions was the same. The rabbit polyclonal antibody against viral antigen and a chicken antisera created against EGFP were used for dual fluorescence. Antibodies

were diluted to 10X the concentration for immunoperoxidase localizations, altering the volume of 0.1 M PO₄ buffer to allow for both antibodies to be in the desired dilution for overnight incubation. After incubation in primary antibodies, the tissue was washed in the same manner as described previously and placed in secondary antibody. Secondary antibodies were Cy2-conjugated donkey anti-chicken or Cy3-conjugated donkey anti-rabbit. Tissue was mounted, dried overnight, passed through graded ethanol and xylenes, coverslipped with Cytoseal-60. The dual-immunofluorescence procedure allowed for localization of neurons containing both the viral antigen demonstrated by an antibody that has been well characterized and used extensively by our laboratory and the farnesylated EYFP reporter by observing the tissue in both the green and red channels.

Endogenous Fluorescence Localization:

Natural fluorescence localization included washing of the tissue to remove cryoprotectant using 6 washes at 10 minutes a wash before mounting on Superfrost microscope slides. Tissue was kept in the dark at 4° centigrade to dry. Coverslips were applied using Vectashield Hard Set mounting media (Vector Labs, Burlingame, CA) and observed immediately.

2.6 Data Collection and Analysis:

The goal of the experiments was to identify circuitry within the spinal cord that can integrate sensory information and communicate it to SPGs through a local circuit network. To first address this question, viral proteins were localized and quantified in a

coronal plane to identify the sequence of infection within each segment. Additionally, the farnesylated EYFP reporter was localized to identify axonal projection patterns.

Sections of the spinal cord were analyzed for infection. After IHC processing using a polyclonal antibody against acetone-inactivated virus, each section of thoracic cord (T1-T13) was analyzed. This antiserum identifies all virally encoded proteins. From each segment, there were approximately 16 sections of spinal cord per bin. Of those sections, the 5 sections with the most labeling within the IML were chosen for quantitative analysis. This approach was chosen because the sympathetic preganglionic neurons that compose the IML do not form a continuous column through each segment. By choosing the 5 most densely labeled sections within each segment we ensured a systematic sampling of each segment that accurately represented the extent of labeling in both the IML and dorsal horn.

Quantitative analysis was completed by counting each infected neuron in the individual lamina and placing these numbers into a spreadsheet. This provided not only a quantity for each segment of spinal cord, but also allowed a determination of the laminar invasion of infection. Laminal boundaries for each segment of the sympathetic cord were determined using Nissl stained tissue, taken from an animal and cytoarchitectural criteria established by Rexed (see figure 5) (Rexed, 1952; 1954). These criteria used cell morphology and packing density of the laminae to establish the ten areas described by Rexed. This cytoarchitecture was used throughout analysis to determine the location of infected cells. Graphs documenting the numbers of infected neurons per spinal cord segment were created to illustrate the dorsoventral as well as rostrocaudal spread of infection.

Figure 5

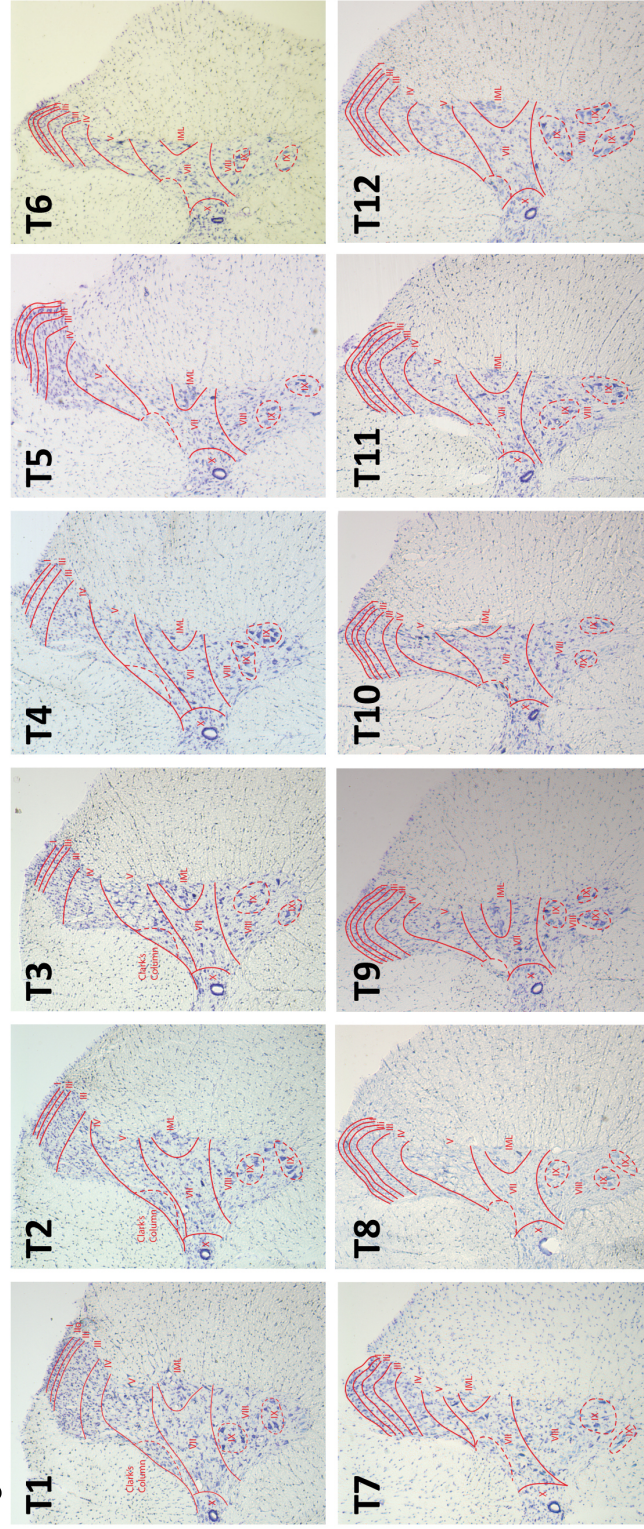


Figure 5: Delineation of Rexed Lamina Boundaries. Boundaries used for mapping of dorsal horn infection were defined on Nissl stained tissue from tissue that was sectioned serially and histochemically marked with Nissl stain. Rexed's original cytoarchitecture descriptions were used for boundary determination.

After determining the spread of infection, it became apparent that neurons in different laminae of the same segment had been infected for differing times, as various stages of infection were apparent in the neurons. To better determine the order in which laminae became infected, each segment was analyzed to determine the stage of infection of neurons within the individual laminae. Infection was determined using the polyclonal rabbit antibody. This antibody identifies numerous viral proteins. Therefore, the differential distribution of viral antigens within infected neurons provides insight into the length of time that the neuron has been replicating virus. Early infection was determined by concentration of viral antigens within the cell nucleus, a distribution reflective of packaging of replicated viral genome within virally coded capsid proteins (see figure 6a). Intermediate infection showed viral proteins within the nucleus and cytoplasm (see figure 6b). Late infection was determined by observation of a dark, homogenous staining within the somatodendritic compartment (see figure 6c). As more viral DNA is transcribed, packed into capsids, and shuttled from the nucleus to the dendrites, the viral antigen is localized further from the nucleus. The life cycle of the virus, used to create these criteria for infection level of individual neurons, has been well documented and described (Card & Enquist, 2012).

Figure 6

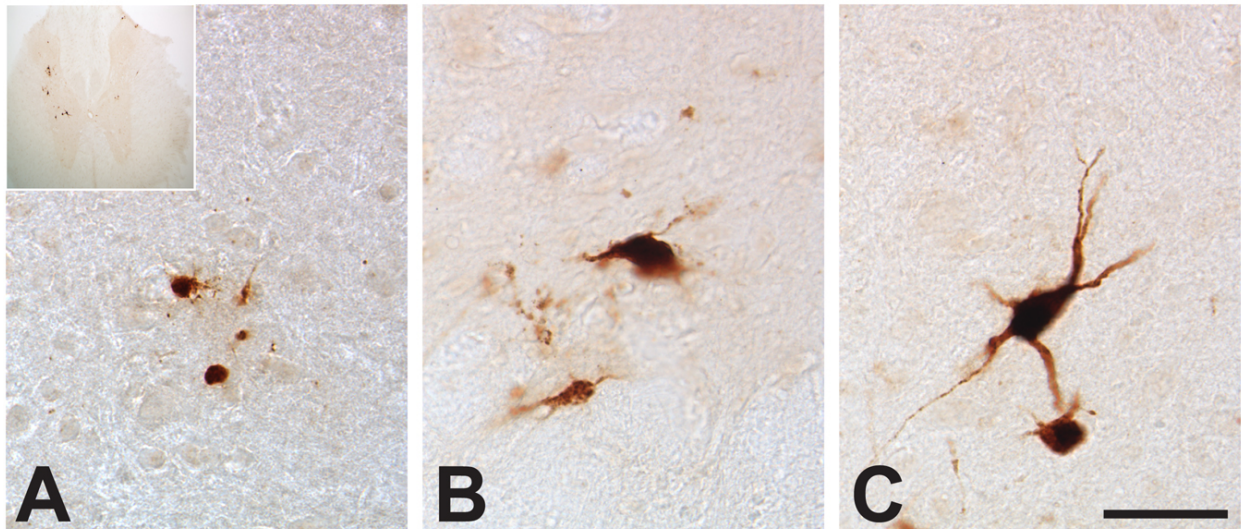


Figure 6. Temporal progression of viral labeling. Neurons in an early stage of infection have viral antigen localized largely confined to the nucleus (A). As the neuron produces more viral progeny, viral antigen is detected within the nucleus and soma of infected neurons (B). The longest infected neurons show label that extends well into the dendritic compartment of neurons (C). The inset image shows a low magnification image of the section from which the viral criteria images were taken. Scale bar=50 um

After staging of infection, it became important to demonstrate the potential pathways of communication for these neurons. The staging allowed us to determine areas in which axonal labeling and arborizations were present. All thoracic segments of the animals injected with PRV279 were processed for the EYFP reporter and each segment was observed for axonal labeling. The axons were mapped using Stereoinvestigator © software followed by photographic documentation using an Olympus microscope. The criteria used to define labeled processes as axons included a non-tapering appearance and the presence of varicosities. In addition to the coronal thoracic segments, horizontal sections of the intermediate portion of the cord, which includes the thoracic segments, were mapped and photographed for evidence of communication between IML pockets within the spinal cord.

DRGs were also observed for fluorescent profile. After careful determination of a potential circuit, presence of EYFP within the DRGs demonstrated that the labeled dorsal horn circuitry received sensory input. DRG tissue was observed for endogenous fluorescent EYFP reporter. Infection was documented photographically.

To gain further insight into the progression of infection within the spinal cord we also analyzed the extent of infection in selected coronal sections of the brain through cell groups known to be synaptically linked to the spinal cord network through descending projections. Given that this is the first use of PRV-279, it was important to define the temporal kinetics of retrograde transneuronal transport of PRV-279 from the kidney. Brain sections were chosen using previous literature to determine neuroinvasiveness of PRV-279. Sections of A5, rostroventral lateral medulla (RVLM), ventromedial medulla (VMM), and paraventricular nucleus of the hypothalamus (PVN)

were chosen. These areas are consistently labeled at a 96-hour postinoculation to PRV-Bartha recombinants and provide accurate measures of viral invasion of renal preautonomic networks (Cano et al, 2004). Brains from animals included in analysis were processed using the rabbit polyclonal antibody against viral antigen. Levels of the brain were chosen using a stereotaxic brain atlas (Swanson, 2004). Nuclei were chosen due to the previous documentation of staining at early post-inoculation times (Cano et al., 2004). Within each nucleus, the level described in the literature to have the highest amount of staining was chosen. Four levels, -12.68 mm, -11.90 mm, -9.50 mm, & +1.78 mm relative to bregma (β), were chosen to determine the viral invasion of the preautonomic network.

Once sections were matched to the appropriate level, sections were mapped using StereoInvestigator software. Sections were outlined using a 2X objective, and then magnification was increased to 40X for neuron counting. Tissue was scanned in rows throughout the entire extent of the section. Any labeled cell was marked if it included a nuclear staining. This criterion eliminated any likelihood of double counting cells between sections. All stages of infection were included in quantitative analysis of the brain.

Infection within the supraspinal targets was used to standardize comparison of viral invasiveness between cases. Postinoculation time is not an adequate indicator for viral infection. Numerous factors contribute to the invasion, replication, and trans-synaptic spread of a virus. The density of innervation of the injection site, the length of the transport, the size of the neuron, and the injection area all contribute to the initial infection of the nervous system, and each factor contributing to initial invasion also

affects transneuronal passage (Card & Enquist, 2012). Using a parenchymal organ, such as the kidney, there are many variables. Each kidney does not exhibit identical innervation patterns and thus, even with identical injections, the viral transport between animals may differ. Therefore, infection of the preautonomic network was used as the marker for infection rate.

3.0 RESULTS

3.1 CONFIRMATION OF PRV279

After analysis in both the brain and spinal cord, the virus is similar to other recombinants of PRV-Bartha. Viral labeling is first seen in lower thoracic levels (T6-T12) at the laminae described in previous literature including IML, V, VII, IV with less extensive labeling in laminae IV, II, & I (Cano et al, 2004). Increasing post-inoculation time showed increased density and level of infection in the lower thoracic levels with the more rostral thoracic levels (T1-T5) showing a delayed infection that appeared similar to early infection in the lower thoracic cord. Supraspinally, infection within the nuclei described in previous research (Cano et al, 2004) shows only a few labeled neurons. Labeling within these regions increases in density as postinoculation time increases.

Several confirmations were completed for the viral reporter protein expression. First, viral proteins were identified with a rabbit polyclonal antibody created against acetone-inactivated PRV virus. This antibody has been shown to label virtually all viral proteins in the genome (Card et al, 1990). The immunoperoxidase labeling showed a pattern of labeling consistent with that expected from a renal injection (Cano et al 2004). To characterize the specific reporter for the virus, an adjacent bin of tissue was stained for EGFP to determine the extent of co-localization between viral antigen

and EGFP. It was shown that the tissue had labeling for EGFP that was in the same regions that had shown the viral protein labeling. Additionally, a third bin of tissue was processed for dual immunofluorescence analysis of viral proteins and EGFP. Using the dual fluorescence analysis, it was shown that the two markers were co-localized in cells (see figure 12). EYFP was only present in neurons that were immunoreactive for viral antigen. However, the viral antigen was detectable prior to the localization of EYFP. Within the neurons, the viral antigens were seen in the soma and dendrites while EGFP was seen in these areas as well in the axons. Axons were distinguished from dendrites by the thin non-tapering projection that was often varicose in appearance.

3.2 QUANTITATIVE ANALYSIS OF VIRAL SPREAD IN THE CORONAL PLANE.

Tissue was sectioned in the coronal plane for a precise laminar and segmental analysis. All segments sectioned in the coronal plane were processed for the viral antigen. The segments were then analyzed by selecting the 5 sections that had the most labeled neurons within the IML. This approach allowed for the least bias in section analysis as it provided a criterion for section analysis. For each section, neurons were counted within each lamina to determine segmental laminar densities. Additionally, the neurons were classified using the conditions established for early, intermediate, and late infection. Using these criteria, total number of neurons within each infection level was separated into 3 divisions, a low, medium, or high number of infected neurons. These numbers were placed into the schematics created from the Nissl stained tissue (see figure 7) and analyzed segmentally between cases, and intersegmentally within cases.

This quantitative approach allowed for analysis of the density, but also brought insight into the circuitry involved in the spinal network.

At the earliest post-inoculation time, infection was seen in the lower thoracic IML and ICN with limited numbers of neurons seen in IML. This is not surprising as these areas are known to contain SPGs would be infected earliest (see figure 8). These neurons innervate the target tissue and would be the route through which virus infects the preautonomic network. At later infection, increased number of neurons and infection level was noted in the IML and ICN in the lower thoracic cord (see figure 8). Labeling was also seen in laminae VII, V, IV, and very light labeling in laminae I & II (see figure 8). This was analyzed quantitatively using stacked graphs of the total infection in each laminae of T10 of one case (see figure 9). These graphs show the total number of infection by bar height, with the laminae differentiated by color. They are stacked in the order in which the lamina became infected.

This spread of virus was evident across cases from early to late infection times. Density of labeling increased in animals with longer post-inoculation times. Each area previously mentioned increased in density as well as level of infection with increased post-inoculation times. IML was seen to have late infected neurons with increasing density at longer post-inoculation times. At the moderate infection periods, labeling was also seen in all laminae of the spinal cord in the lower thoracic (T6-T13) with increasing density in the caudal portion of the cord (see figure 10).

Figure 7

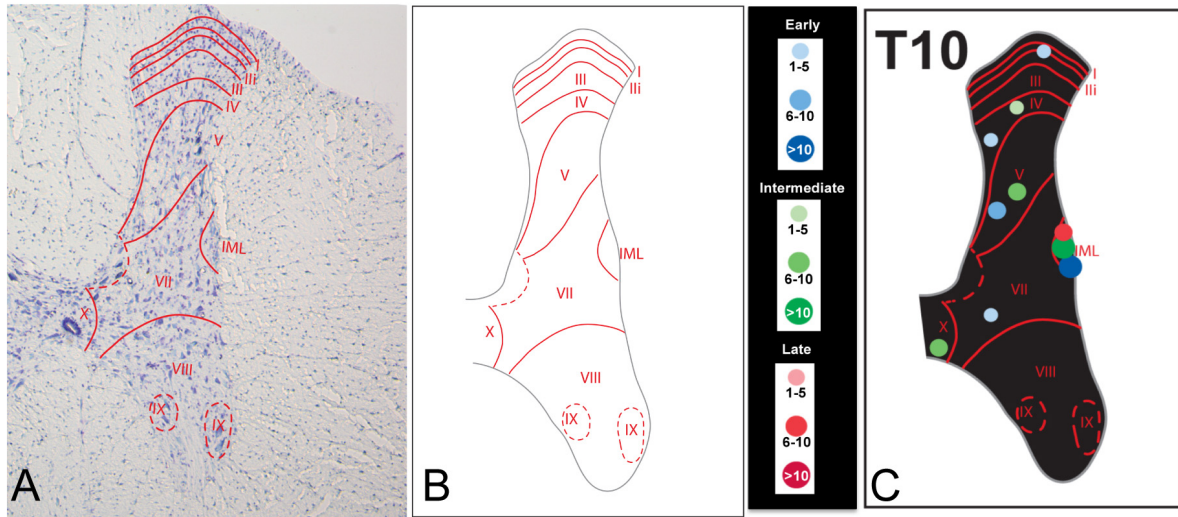


Figure 7: Schematic Representation of Sympathetic Spinal Cord Segments. Using Nissl stained tissue were delineated using Rexed's cytoarchitonic criteria (A). These maps then were made into schematics for representation of viral localization (B). Infection level was determined and plotted using differing colors. The number of neurons of each infection level was differentiated using size of the marker as an indicator.

Figure 8

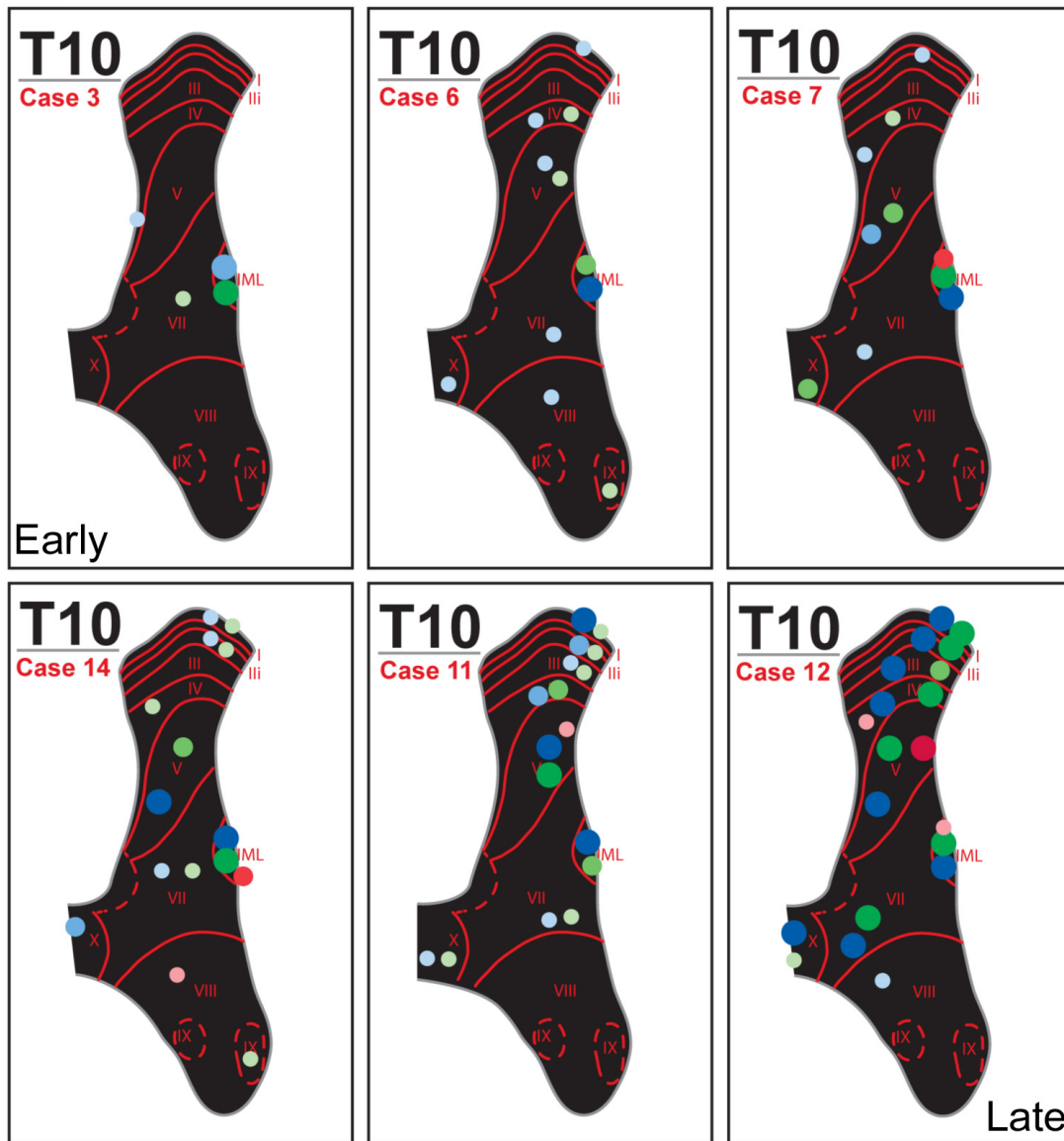


Figure 8: Schematic Representation of Preautonomic Network Viral Labeling. Viral antigen was present at early infection within the IML. Longer infection periods showed labeling within laminae V, VII, IV and light infection of I & II. These areas increased in density and infection level as infection period increased. Circumscribed populations of neurons were noted in all infection periods studied.

Figure 9

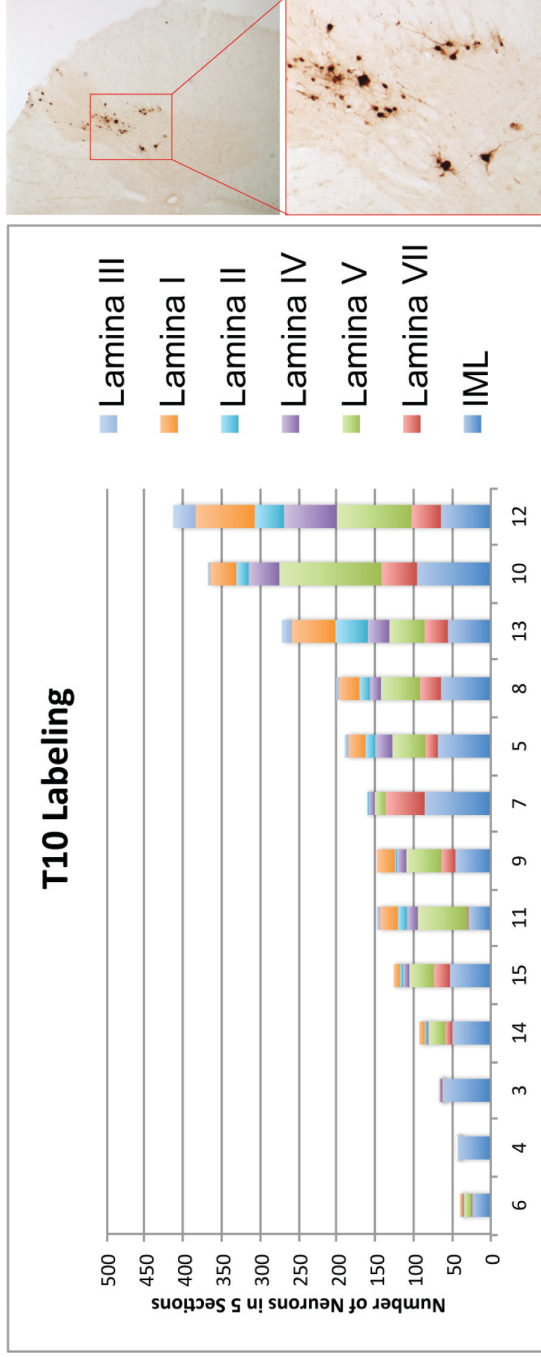


Figure 9. Labeling in Spinal Segment T10. Early infection periods showed labeling within the IML and limited spread. Increasing number of neurons in the IML also shows labeling in the dorsal horn laminae including laminae I, II, IV, V, & VII. This infection increased as infection periods increased. Even at long infection periods, the labeling is restricted to a subset of neurons within the laminae as seen in the photomicrograph from case 10 T10. Cases are ordered from early to latest infection along the horizontal axis.

Figure 10

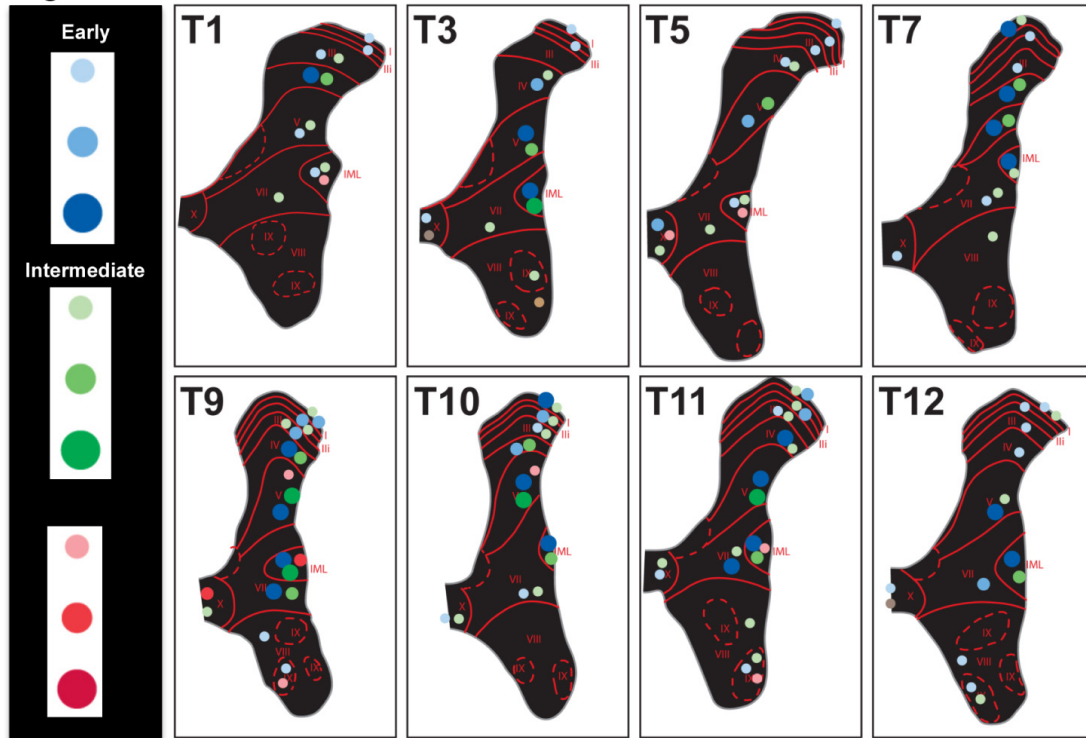


Figure 10: Intersegmental Invasion of Preautonomic Networks. Infection in the caudal thoracic spinal cord followed a temporally delayed invasion of the dorsal horn. Rostral thoracic segments became infected at longer infection periods. Importantly, the circuitry in the rostral thoracic segments recapitulated the pattern of infection seen at the caudal levels.

At the latest infection level, several things were noted. There was a decrease in the labeling of the IML in the lower thoracic spinal cord (see figure 9 case 12). Increasing density of infection was observed in the dorsal horn of the spinal cord in all levels of infection. This density increased across the laminar divisions, but the proportion of labeling within each lamina appeared similar across levels of infection, in that, once a lamina became infected, the relative proportion of infection present within that lamina stayed similar (see figure 9). Additionally, the ventral horn increased in labeling density, as did lamina X (CAN) and ICN. This was true for all levels of the thoracic cord. In addition, viral protein was localized within the DRG of the lower thoracic segments (see figure 12). Regardless, increased level of infection was seen in all laminar divisions.

Figure 11

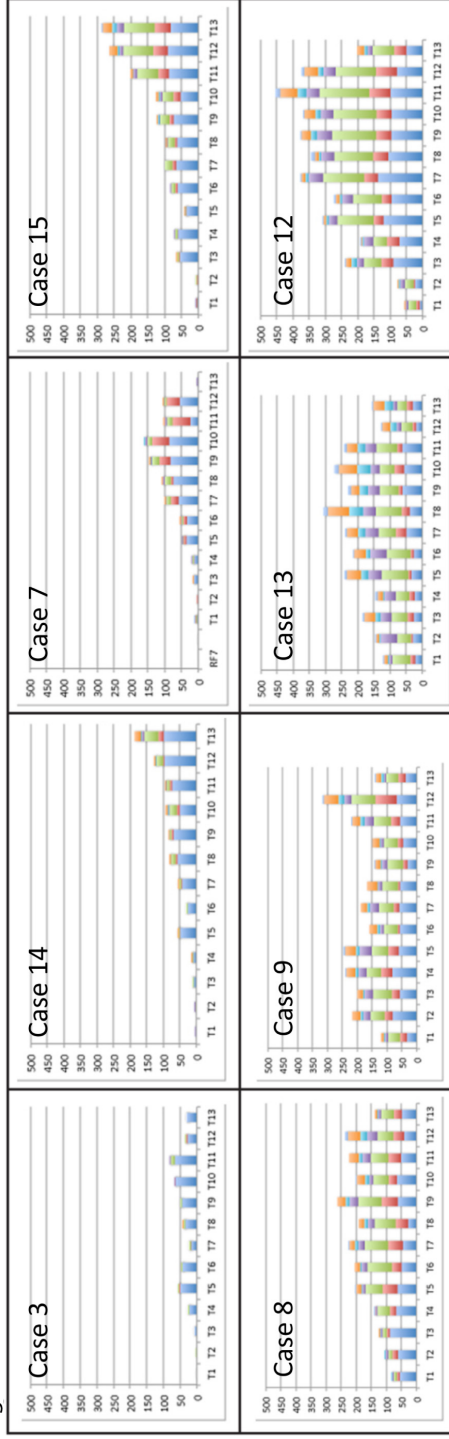


Figure 10: Infection of Laminae Across Thoracic Segments. As infection periods increased, the number of infected neurons also increased. This was present first in the caudal thoracic spinal cord and spread to more rostral segments at longer infection time. Total number of neurons increased in each segment and once infected, number of neurons within individual laminae was apparent in a similar relative proportions. Color identification found on Figure 9.

Figure 12

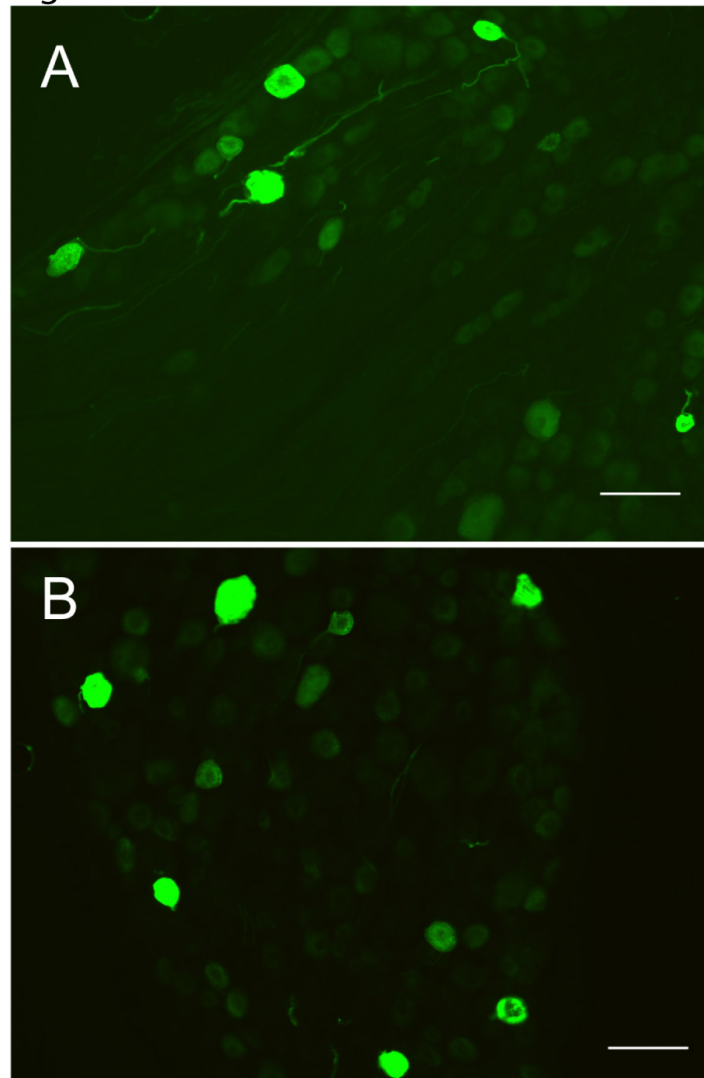


Figure 12: Infection in Sensory Afferents. Within DRGs of the caudal thoracic cord of late infection periods, EYFP is observed. This labeling was present and implicates sensory afferents to the circuitry, as these are the neurons present within the DRG. Scale Bar= 50 μm

3.3 PRV279 ANALYSIS OF AXONAL PROJECTIONS.

Axonal projections were analyzed using the farnesylated EYFP reporter. The farnesyl group allows for a more complete analysis of cell morphology. Tissue taken from the same animal processed using the viral antigen in one bin with a second bin processed for EGFP (see figure 13). These sections, from the same animal, show the advantages of both antibodies. The viral antisera shows the labeling necessary for infection staging, while the EGFP shows the entire dendritic tree as well as axonal arborizations (see figure 14).

Projections of axons and dendrites were co-existent with populations of neurons labeled with PRV279. In the coronal plane, numerous axons were seen coursing from the SDH to the deeper dorsal horn. Additionally, axons were seen projecting between lamina IV to laminae V & VII, as well as neurons within laminae V & VII projecting into the IML (see figure 14). In addition, axons were seen projecting bilaterally confirming previous findings that suggests a coordinated sympathetic circuit within the spinal cord (Cano et al, 2004).

Horizontal analysis was performed to identify additional possible routes of viral transport. It has been suggested that rostrocaudal spread of virus occurs through the chain ganglia of the PNS. Interestingly, numerous examples of axons were noted that coursed between pockets of IML labeling (see figure 15). Similar patterns of axonal projections in the rostrocaudal plane were also observed in the mouse, showing conservation across species. These rostrocaudal projections are indicative of a parallel pathway to the chain ganglia that occurs strictly within the spinal cord.

Figure 13

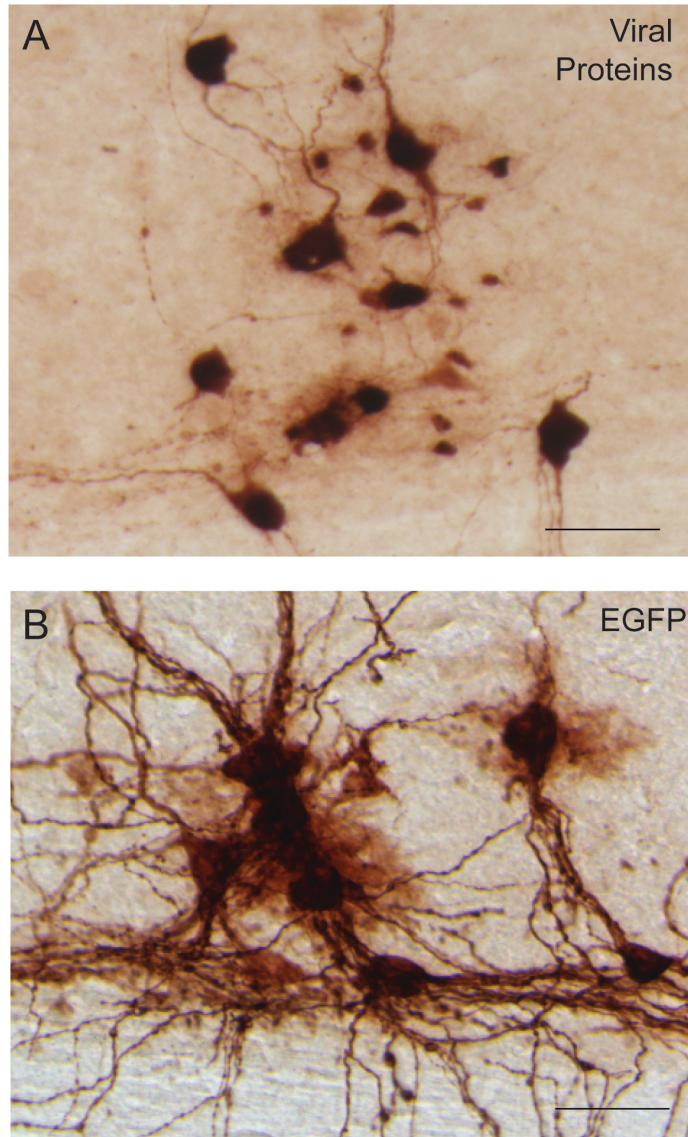


Figure 11: Comparison of Viral Antigen and EGFP Immunoperoxidase Staining. Viral protein labeling was localized in a longitudinal section of spinal cord. All stages of infection are observed (A). In an adjacent bin of tissue, an antibody against EGFP which labels the farnesylated EYFP reporter is localized. The EGFP localization allows for a more complete morphological profile (B). Scale bar=50 μ m

Figure 14

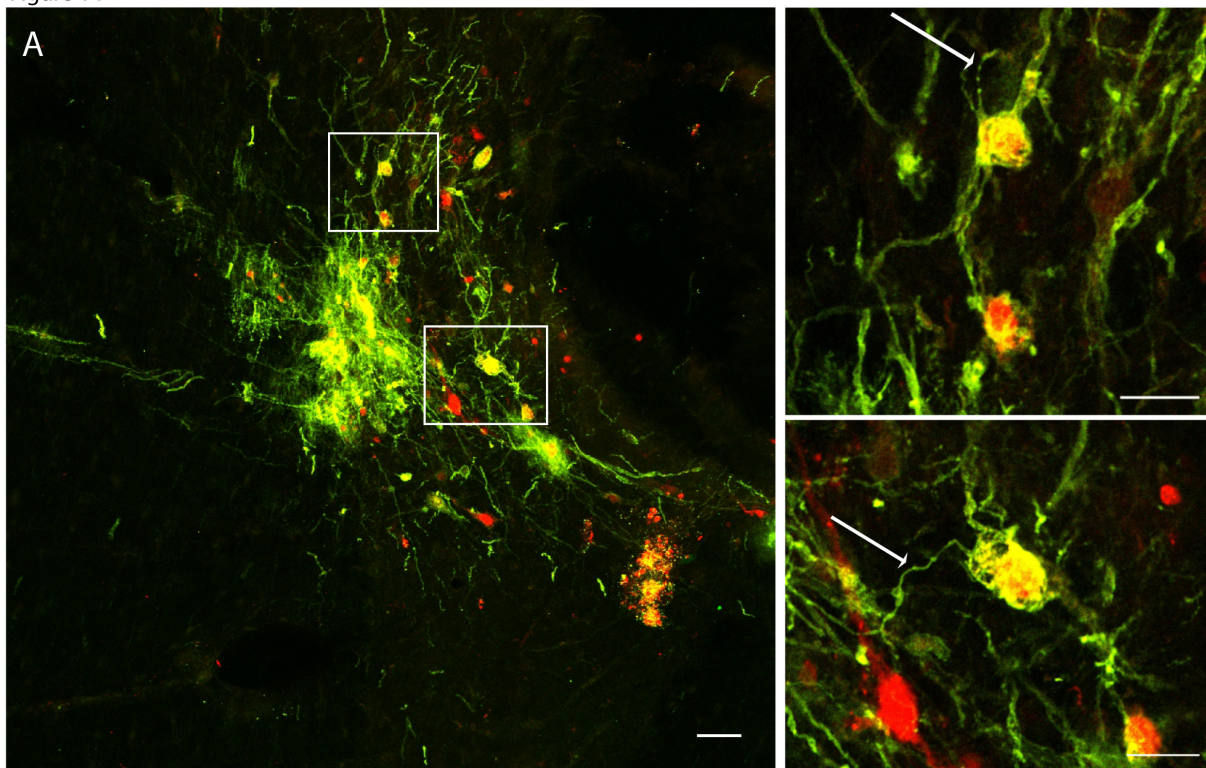


Figure 12: Axonal Projections in the Dorsal Horn. A confocal microscopic maximum projection image through an IML pocket within thoracic segment 9 shows evidence of axonal projections within the dorsal horn (A). Viral antigen is localized with a red fluorescent tag, while EYFP was localized with the green fluorescent tag. Numerous cases of axons are seen with thin, non-tapering projections and the presence of buttons of passage (top right image). Additionally, axons were seen projecting from areas previously determined as populations of INs into the IML (bottom right image). Scale bar= 50 μ m

Figure 15

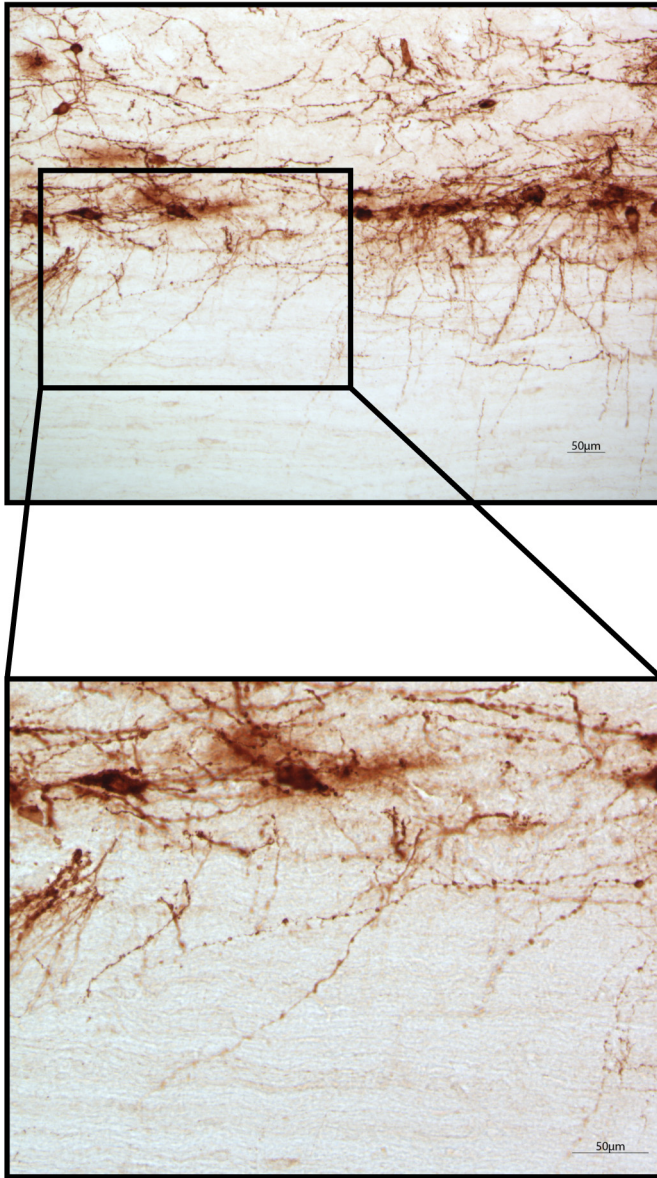


Figure 13: Axonal Labeling in the Longitudinal Plane. Axons were seen coursing rostrocaudally between all labeled IML pockets as evidenced by thin, non-tapering projections that displayed a varicose appearance. Scale bar=50um

4.0 DISCUSSION

The present study confirms many findings of research in current literature, while adding new observations. New technology in the form of a PRV strain that expresses a farnesylated EYFP reporter was carefully characterized prior to use in these experiments. The novel strain of PRV replicates and invades similar to other PRV-Bartha recombinants. First, spinal cord labeling occurred fairly early in postinoculation time at 72 hours which is similar to previous reports (Cano et al, 2004). Additionally, at late postinoculation periods, viral labeling was apparent in the brain in regions previously shown to be infected by 120 hr post-inoculation time, including the LC, A5, VMM, RVLM, and PVN (Cano et al, 2004). The fluorescent reporter profile shows an endogenous EYFP reporter demonstrating the expression of the reporter protein from the genome. The EYFP reporter showed a delayed expression when compared to the viral antigen. The reporter was observed in all compartments of the neuron including the soma, dendrites, and axons, indicating the presence of the farnesylation and impregnation of the membrane. Overall, the data suggest that the virus invades, replicates, and passes transneuronally similar to other PRV-Bartha recombinants and can be used as a novel strain of PRV due to the hydrophobic tendencies of the fluorescent reporter.

The segmental analysis of labeling in the thoracic spinal cord in a coronal plane provided novel insight into the organization of a sympathetic circuit. In a single segment of caudal thoracic spinal cord, SPNs become labeled first, followed by laminae V, VII, & IV, with laminae I & II infected but with a lower quantity of labeled neurons than the deeper dorsal laminae. These findings are consistent with previous research using tracing and electrophysiological techniques (Cabot et al., 1994; Clarke et al., 1998; Cano et al., 2001; Brooke et al., 2002; Tang et al., 2004; Cano et al., 2004). This early replication and invasion of virus to all laminae suggest an interneuron that is presynaptic to the SPGs due to the labeling presence and infection stage of subsets of infected neurons.

At increasing infection rates, labeling in previously infected laminae increased. Additionally, the presence of varying infection levels shows an increase in early infections in the dorsal horn, while showing intermediate and late labeling in the deeper dorsal horn. This temporally delayed and segregated viral labeling is suggestive of a progressive pathway in which laminae I & II interneurons project to interneurons within laminae V, VII, & IV, which, in turn, innervate SPNs in the IML. This is shown by the delay of later infection stages as well as number of infected neurons (see figure 11). Additionally, previous tract tracing research has shown evidence for interneurons presynaptic to SPGs found in deeper dorsal horn laminae (Cabot et al., 1994; Clarke et al 1998; Tang et al, 2004). Because there is labeling using a tracer that does not self-amplify (Cabot et al 1994) as well as short post inoculation times in transneuronal tracers (Clarke et al 1998; Tang et al 2004), there is support of a dense innervation from these deeper laminae to the SPGs in the IML. Laminae I & II may not have been

detected in earlier studies due to differences in tracers and postinoculation periods. However, the presence of infected neurons at early infection periods suggests the presence of a direct projection from neurons in laminae I & II to SPGs in the IML (see figure 16A).

Additionally, a sequential projection from the sensory afferents synapsing upon interneurons within the thoracic spinal cord dorsal horn, which in turn innervate the SPGs, is suggested by the data. This polysynaptic circuit allows for a population that may be integrated with other modulatory influences, either from other segments of spinal cord, or supraspinal innervation. The presence of labeling within the deeper dorsal horn laminae in previous tract tracing studies would suggest a population in the deeper laminae (Cabot et al., 1994; Clarke et al 1998; Tang et al, 2004), however electrophysiological data has correlated IN activity laminae I, II, & III with sympathetic outflow as well (Miller et al 2001; Tang et al, 2003). This polysynaptic circuit would show not only the labeling that is described in the literature, but also a population antecedent to those within laminae V, VII, & IV that would show a correlation to activity.

The data, when interpreted in the context of the literature, suggests a direct pathway in which a sensory afferent synapses upon an IN in the dorsal horn, which in turn innervates the SPGs in the IML (see figure 16a). A secondary polysynaptic pathway is also suggested by the data, in which sensory afferents synapse upon INs within the dorsal horn, which then projects to INs in laminae V, VII, or IV (see figure 16b). These INs within the deeper dorsal laminae would then innervate SPGs to alter sympathetic outflow. Analysis of axonal labeling using the farnesylated reporter support

the presence of this segmental circuit. These are two of the potential routes of infection and are not the only potential circuits.

Other segments of the spinal cord may become infected by different routes. First, data using the farnesylated virus and a horizontal plane of spinal cord show axons coursing between segments of IML (see figure 15). Therefore, one possibility is that the SPNs or INs of the IML are coordinating outflow rostrocaudally within the spinal cord, without using any nodes between them (see figure 17 dashed red line). A second possibility is that the SPNs of higher thoracic levels may become labeled through the sympathetic chain ganglia (see figure 17). This labeling would then label the IML first, and follow in a similar temporal delay on upper dorsal horn labeling. Axons are seen coursing rostrocaudally within the spinal cord between all labeled IML segments. This provides evidence of a circuit within the spinal cord that is a possible source of integration across segments for coordinated sympathetic outflow.

Functionally, there are numerous advantages to a sympathetic circuit within the spinal cord. First, a sensory afferent causing sympathetic outflow with minimal number of synapses allows for a faster acting response to reestablish homeostasis. This is beneficial for an organism for survival, as the quicker prey respond to a predator, the better likelihood of living through a potential attack. The suggestion of multiple circuits allowing sensory information to relay to SPGs allows for this rapid alteration in sympathetic outflow as well as a population that is subject to modulation allows for a rapid yet precise alteration in sympathetic outflow.

Figure 16

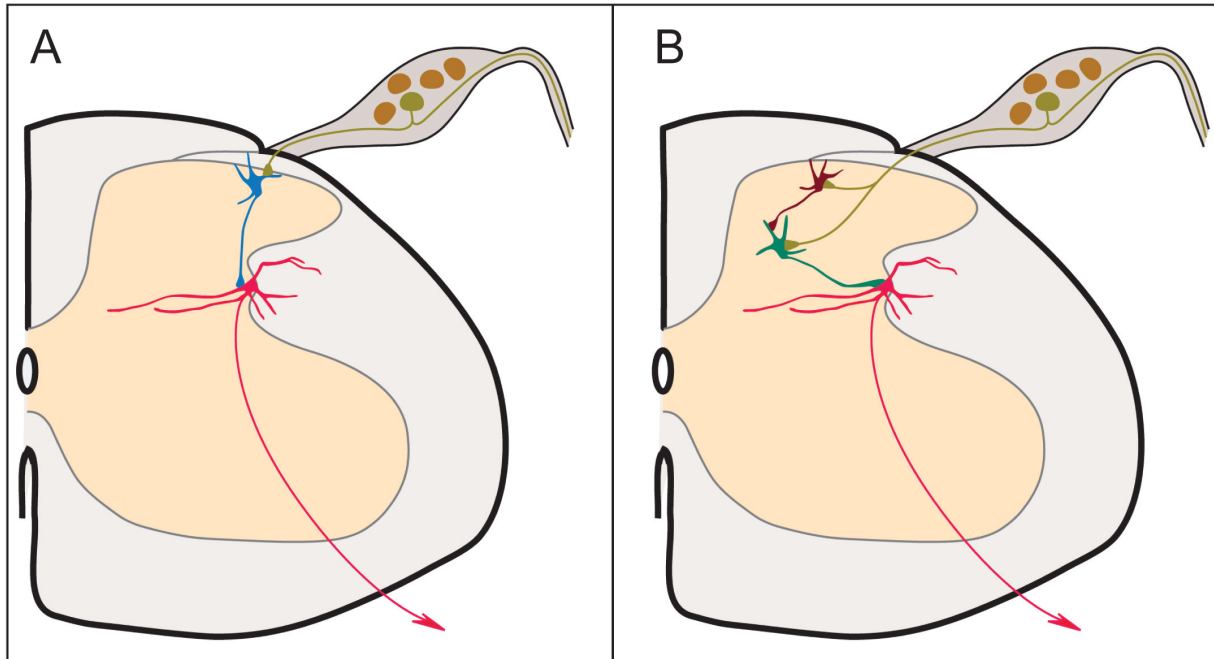


Figure 14. Schematic Diagram of Segmental Circuitry. The data are consistent with two proposed circuits. One circuit is a connection from the sensory afferent onto an interneuron that then innervates SPGs in the IML as indicated by early labeling in the superficial layers (A). A secondary circuit proposed by viral invasion provides a more indirect route of modulation. Sensory afferents innervate interneurons within the dorsal horn that may integrate inputs from within the segments, intersegmentally, and descending from supraspinal nuclei (B).

Figure 17

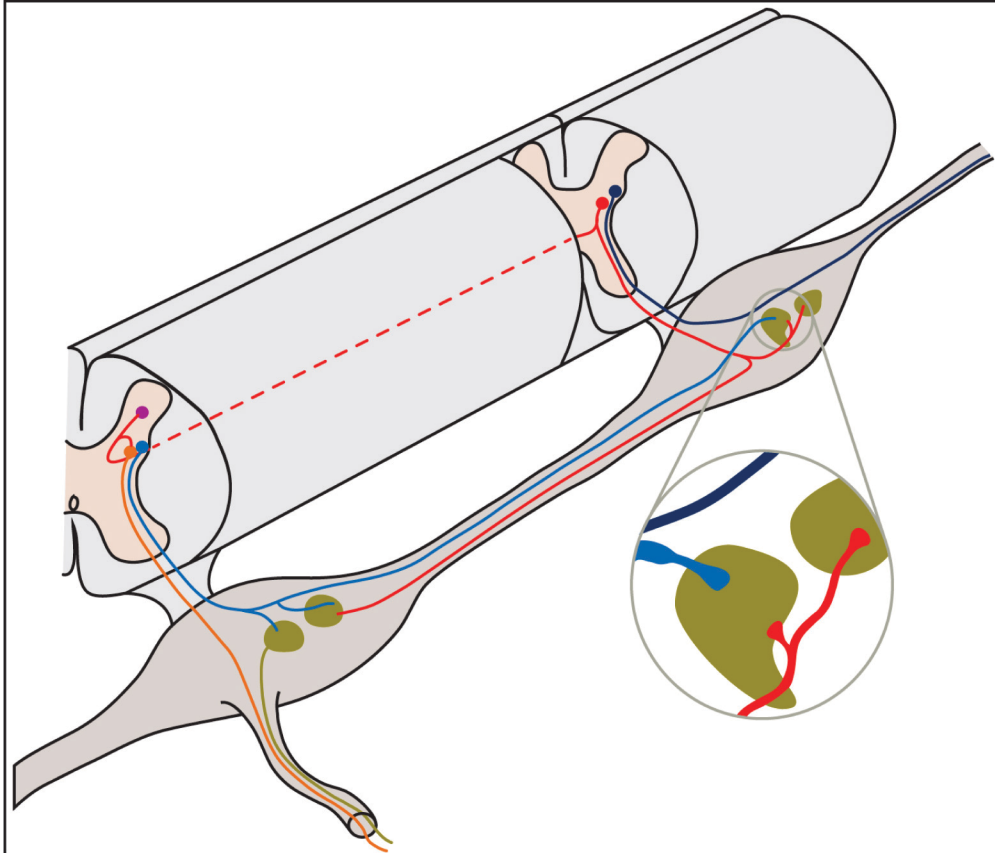


Figure 15. Intersegmental Coordination of Sympathetic Outflow.

Axonal projections demonstrated by the farnesylated virus suggest a parallel circuitry to that of the paravertebral chain. This parallel circuit projects rostrocaudally between IML segments. This parallel circuit provides a second circuit for coordinated outflow.

Additionally, an integrative circuit is a strong evolutionary advantage. The outflow from the CNS to the peripheral targets is complementary across varying organs and thus requires synchronization across the body. Synchronization is not a novel concept. Another such reflex requiring coordination is the flexor reflex. When a person steps on a tack, A δ fibers bring sensory information into the spinal cord. These afferents synapse upon interneurons in the cord. Interneurons cause the quadriceps (flexor) muscle to contract through an excitatory process. A different primary interneuron sends a GABAergic projection to the hamstring (extensor) and this complementing pathway causes the person to lift their foot in response to the tack (Nicholls et al, 2001). The proposed circuit is separate from the reflex described above, but has a similar effect in which the pathways within the spinal cord that coordinate outflow would support a system wide change of the sympathetic outflow in times of challenge. This circuit would receive a collateral from the primary afferent as well, which would cause the change in homeostatic status, increasing blood flow to the muscles and respiratory rate for example, to adjust for this motor reflex. Additionally, evidence of this rostrocaudal projection was present in both the mouse and rat, suggestive of a circuit preserved across species.

This study builds on previous work by providing a longer post-inoculation time than has previously been included in a coronal plane. The careful, detailed temporal analysis allows a proposed circuit to be determined using axonal projections as additional support for the circuit proposed from the viral invasion data. Using the level of infection and number of neurons, one proposed circuit shows a primary afferent into the dorsal horn laminae I & II, synapsing upon an interneuron which in turn projects to

deeper dorsal and intermediate horn laminae V, VII, & IV. These secondary interneurons project to the IML, either synapsing upon SPNs or INs known to exist in the population. A second circuit suggested is a sensory afferent synapsing upon neurons in the dorsal horn which then innervate SPGs.

The findings of the current study must be more fully characterized in future experiments. The first step towards a better understanding of the circuit is the phenotypic identity of the class of neurons that are presympathetic in the dorsal horn. Knowledge of the phenotype of the neurons antecedent to SPGs would allow for a more informed analysis of the consequence of an action potential from a lamina I interneuron on the IML neuron onto which it synapses.

Additionally, it is possible that labeling within the DRGs results from retrograde transport of virus from the kidney rather than via retrograde transneuronal transport through a dorsal horn circuit linked to SPGs. To analyze the potential for DRG labeling occurring through the sensory afferent, rather than through the spinal cord dorsal horn, a second experiment is needed. The experiment would need to be replicated with animals also receiving a transection of the dorsal root immediately distal to the ganglion. This would eliminate the fear of any DRG labeling arising from the sensory afferent.

While numerous steps are necessary to fully illuminate the sympathetic spinal cord circuitry, the detailed quantitative approach employed in the current experiment answered many key points of interest. First, the spinal cord interneuron population expands beyond what has been described in the literature to include numerous neurons within the SDH. Second, these INs provide a avenue for sensory afferents to gain access to autonomic outflow at the level of the spinal cord as there are labeled neurons

within the DRGs of late infected thoracic segments. Additionally, there are neurons within the IML that project rostrocaudally between ipsilateral thoracic IML segments, which has previously been thought to occur only through chain ganglia. Lastly, there is evidence for both a parallel and sequential pathway through the dorsal horn of the spinal cord, connecting dorsoventrally as well as rostrocaudally. This study adds an additional piece to the sympathetic circuitry within the spinal cord using a detailed analysis of infection densities, levels of infection, and axonal mapping to provide one of the most detailed descriptions of the spinal dorsal horn circuitry to date.

LITERATURE CITED

- Anderson CR & Edwards SL. Intraperitoneal injections of Fluorogold reliably labels all sympathetic preganglionic neurons in the rat. *Journal of Neuroscience Methods* 1994; 53(2): 137-41
- Blottner D, Baumgarten HG. Nitric oxide synthetase (NOS)-containing sympathoadrenal cholinergic neurons of the rat IML-cell column: Evidence from histochemistry, immunohistochemistry, and retrograde labeling. *Journal of Comparative Neurology* 1992; 316(1): 45-55.
- Brooke RE, Pyner S, McLeish P, Buchan S, Deuchars J, Deucars SA. Spinal cord interneurons labelled transneuronally from the adrenal gland by a GFP-herpes virus construct contain the potassium channel subunit Kv3.1b. *Autonomic Neuroscience* 2002; 98(1-2): 45-50.
- Cabot JB, Alessi V, Carroll J, Ligorio M. Spinal cord lamina V and lamina VII interneuronal projections to sympathetic preganglionic neurons. *Journal of Comparative Neurology* 1994; 342(4): 515-30.
- Cano G, Sved AF, Rinaman L, Rabin BS, Card JP. Characterization of the central nervous system innervation of the rat spleen using viral transneuronal tracing. *Journal of Comparative Neurology* 2001; 439(1): 1-18.
- Cano G, Card JP, Sved AF. Dual viral transneuronal tracing of central autonomic circuits involved in the innervation of the two kidneys in rat. *Journal of Comparative Neurology* 2004; 471(4): 462-81.
- Card JP, Rinaman L, Schwaber JS, Miselia RR, Whealy ME, Robbins AK, Enquist LW. Neurotropic properties of pseudorabies virus: Uptake and transneuronal passage in the rat central nervous system. *Journal of Neuroscience* 1990; 10(6) 1974-94.
- Card JP, Rinaman L, Lynn RB, Lee BH, Meade RP, Miselis RR, Enquist LW. Pseudorabies virus infection of the rat central nervous system: Ultrastructural characterization of viral replication, transport, and pathogenesis. *Journal of Neuroscience* 1993; 13(6): 2515-39.

- Card JP, Kobiler O, McCambridge J, Ebdlahad S, Shan Z, Raizada MK, Sved AF, Enquist LW. Microdissection of neural networks by conditional reporter expression from a Brainbow herpesvirus. *Proceedings of the National Academy of Sciences* 2011; 108(8): 3377-82.
- Card JP & Enquist LW. Use and visualization of neuroanatomical viral transneuronal tracers. *Visualization Techniques: From Immunohistochemistry to Magnetic Resonance Imaging*, Badoer E (ed.) *Neuromethods* 2012; 70: 225-68.
- Chau D, Kim N, Schramm LP. Sympathetically correlated activity of dorsal horn neurons in spinally transected rats. *Journal of Neurophysiology* 1997; 77(6): 2966-74.
- Chau D, Johns DG, Schramm LP. Ongoing and stimulus-evoked activity of sympathetically correlated neurons in the intermediate zone and dorsal horn of acutely spinalized rats. *Journal of Neurophysiology* 2000; 83(5): 2699-707.
- Clarke HA, Dekaban GA, Weaver LC. Identification of lamina V and VII interneurons presynaptic to adrenal sympathetic preganglionic neurons in rat using recombinant herpes simplex virus type 1. *Neuroscience* 1998; 85(3): 863-72.
- Deuchars SA, Brooke RE, Frater B, Deuchars J. Properties of interneurons in the Intermediolateral cell column of the rat spinal cord: Role of the potassium channel subunit Kv3.1. *Neuroscience* 2001; 106(2): 433-46.
- Deuchars SA, Milligan CJ, Stornetta RL, Deuchars J. GABAergic neurons in the central region of the spinal cord: A novel substrate for sympathetic inhibition. *Journal of Neuroscience* 2005; 25(5): 1063-70.
- Joshi S, Levatte MA, Dekaban GA, Weaver LC. Identification of spinal interneurons antecedent to adrenal sympathetic preganglionic neurons using trans-synaptic transport of herpes simplex type 1. *Neuroscience* 1995; 65(3): 893-903.
- Kerman IA, Enquist LW, Watson SJ, Yates BJ. Brainstem substrates of sympatho-motor circuitry identified using trans-synaptic tracing with pseudorabies virus recombinants. *Journal of Neuroscience* 2003; 23 (11): 4657-66.
- Kobiler O, Lipman Y, Therkelsen K, Daubechies I, Enquist LW. Herpesviruses carrying a Brainbow cassette reveal replication and expression of limited numbers of incoming genomes. *Nature Communications* 2010; 146 (1): 1-8.
- Krassioukov AV, Johns DG, Schramm LP. Sensitivity of sympathetically correlated interneurons, renal sympathetic nerve activity, and arterial pressure to somatic and visceral stimuli after chronic spinal injury. *Journal of Neurotrauma* 2002; 19(12): 1521-9.

- Livet J, Weissman TA, Kang J, Draft RW, Bennis RA, Sanes JR, Lichtman JW. Transgenic strategies for combinatorial expression of fluorescent proteins in the nervous system. *Nature* 2007; 450(7166) 56-62.
- Llewellyn-Smith IJ, Cassam AK, Krenz NR, Krassioukov AV, Weaver LC. Glutamate- and GABA-immunoreactive synapses on sympathetic preganglionic neurons caudal to a spinal cord transection in rats. *Neuroscience* 1997; 80(4): 1225-35.
- Llewellyn-Smith IJ & Weaver LC. Changes in synaptic inputs to sympathetic preganglionic neurons after spinal cord injury. *Journal of Comparative Neurology* 2001; 435(2): 226-40.
- Llewellyn-Smith IJ, Dicarlo SE, Collins HL, Keast JR. Enkephalin-immunoreactive interneurons extensively innervate sympathetic preganglionic neurons regulating the pelvic viscera. *Journal of Comparative Neurology* 2005; 488(3): 278-89.
- Llewellyn-Smith IJ, Martin CI, Fenwick NM, Dicarlo SE, Lujan HL, Schrelhofer AM. VGLUT1 and VGLUT2 innervation in autonomic regions of intact and transected rat spinal cord *Journal of Comparative Neurology* 2007; 503(6): 741-67.
- Marty J, Gauzit R, Lefevre P, Couderc E, Henzel C, Desmonts JM. Effects of diazepam and midazolam on baroreflex control of heart rate and on sympathetic activity in humans. *Anesthesia and Analgesia* 1986; 65(2): 113-9.
- McLean IW & Nakane PK. Periodate-lysine-paraformaldehyde fixative. A new fixation for immunoelectron microscopy. *Journal of Histochemistry and Cytochemistry* 1974; 22(12): 1077-83.
- Miller CO, Johns DG, Schramm LP. Spinal interneurons play a minor role in generating ongoing renal sympathetic nerve activity in spinally intact rats. *Brain Research* 2001; 918(1-2): 101-6.
- Nicholls JG, Martin AR, Wallace BG, Fucks PA (eds.). *From Neuron to Brain* 4th edition. Sunderland, MA: Sinauer Associates, Inc.: 2001.
- Otis TS, Staley KJ, Mody I. Perpetual inhibitory activity in mammalian brain slices generated by spontaneous GABA release. *Brain Research* 1991; 545(1-2): 142-50.
- Rexed B, The cytoarchitectonic organization of the spinal cord in the cat. *Journal of Comparative Neurology* 1952; 96(3): 414-95.
- Rexed B, A cytoarchitectonic atlas of the spinal cord in the cat. *Journal of Comparative Neurology* 1954; 100(2): 297-379.

- Rinaman L, Card JP, Schwaber JS, Misells, RR. Ultrastructural demonstration of a gastric monosynaptic vagal circuit in the nucleus of the solitary tract. *Journal of Neuroscience* 1989;9(6):1985-96.
- Schramm LP, Strack AM, Platt KB, Loewy AD. Peripheral and central pathways regulating the the kidney: a study using pseudorabies virus. *Brain Research* 1993; 616(1-2): 251-62.
- Swanson LW. *Brain Maps: Structure of the Rat Brain*. Amsterdam: Elsevier; 2004.
- Taneyama C, Goto H, Kohno N, Benson KT, Sasao J, Arkawa K. Effects of fentanyl, diazepam, and the combination of both on arterial baroreflex and sympathetic nerve activity in intact and baro-denervated dogs. *Anesthesia and Analgesia* 1993; 77(1): 44-8.
- Tang X, Neckel ND, Schramm LP. Locations and morphologies of sympathetically correlated neurons in the T(10) spinal segment of the rat. *Brain Research* 2003; 976(2): 185-93.
- Tang X, Neckel ND, Schramm LP. Spinal interneurons infected by renal injection of pseudorabies virus in the rat. *Brain Research* 2004; 1004(1-2): 1-7.
- Wang L, Spary E, Deuchars J, Deuchars SA. Tonic GABAergic inhibition of sympathetic preganglionic neurons: A novel substrate for sympathetic control. *Journal of Neuroscience* 2008; 28(47): 12445-52.
- Watson RE Jr, Wiegand SJ, Clough RW, Hoffman GE. Use of cryoprotectant to maintain long-term peptide immunoreactivity and tissue morphology. *Peptides* 1986; 7(1): 155-9.